Received: 9 March 2023 | Accepted: 26 September 2023

DOI: 10.1111/pce.14733

ORIGINAL ARTICLE

Plant, Cell & Environment | WILEY

Bark water uptake through lenticels increases stem hydration and contributes to stem swelling

Holly A. A. Beckett[1] | Daryl Webb[2] | Michael Turner[3] | Adrian Sheppard[3] | Marilyn C. Ball[1]

[1]Plant Science Division, Research School of Biology, Australian National University, Canberra, Australia

[2]Centre for Advanced Microscopy, Australian National University, Canberra, Australia

[3]Department of Applied Mathematics, Research School of Physics, Australian National University, Canberra, Australia

Correspondence
Holly A. A. Beckett, Plant Science Division, Research School of Biology, Australian National University, Canberra, ACT 2601, Australia.
Email: Holly.beckett@anu.edu.au

Funding information
Australian Government Research Training Program; National Collaborative Research Infrastructure Strategy; Australian Research Council

Abstract

Foliar water uptake can recharge water storage tissue and enable greater hydration than through access to soil water alone; however, few studies have explored the role of the bark in facilitating water uptake. We investigated pathways and dynamics of bark water uptake (BWU) in stems of the mangrove *Avicennia marina*. We provide novel evidence that specific entry points control dynamics of water uptake through the outer bark surface. Furthermore, using a fluorescent symplastic tracer dye we provide the first evidence that lenticels on the outer bark surface facilitate BWU, thus increasing stem water content by up to 3.7%. X-ray micro-computed tomography showed that BWU was sufficient to cause measurable swelling of stem tissue layers increasing whole stem cross-sectional area by 0.83 mm^2 or 2.8%, implicating it as a contributor to the diel patterns of water storage recharge that buffer xylem water potential and maintain hydration of living tissue.

KEYWORDS
bark water uptake, lenticel, mangrove, salinity, stem swelling, water storage

1 | INTRODUCTION

Both carbon gain and turgor are essential for plant function, growth and survival. Carbon cannot be gained without water loss, while turgor cannot be generated without maintaining hydration. However, extreme temperatures, drought and evapotranspiration associated with climate change are increasing demand for water use and reducing water availability, leading to a global increase in plant mortality (Allen et al., 2010; Breshears et al., 2013; Grossiord et al., 2020; McDowell et al., 2022). For example, the widespread mangrove mortality seen across Australia in 2015–16 was coincident with an extreme El Niño event (Abhik et al., 2021; Duke et al., 2017; Harris et al., 2018; Lovelock et al., 2017; Lucas et al., 2018). Understanding the multiple sources of water a plant may access to maintain hydration is essential to identifying the limitations imposed on plant function and survival when water availability declines and demand for water increases.

Increasingly, studies have shown that foliar water uptake (FWU), the movement of atmospheric water into leaves, substantially improves whole plant hydration, and even increases hydration of the rhizosphere (Dawson & Goldsmith, 2018; Eller et al., 2013; Schreel & Steppe, 2020; Simonin et al., 2009). However, FWU may not be the only pathway for top-down rehydration. There is evidence that absorption of atmospheric water also occurs through the outer bark surface of stems (phellem). Bark water uptake (BWU) has been found to reduce tracheal embolism, partially restore hydraulic conductivity, and increase stem water potential (Katz et al., 1989; Liu et al., 2019; Mason Earles et al., 2016). Therefore, BWU may play

a role in maintaining hydraulic function and carbon gain. Yet few studies have directly tested for BWU.

In a literature search, we found only 11 studies that measured liquid water uptake from wet stem surfaces. Of these, two did not differentiate between FWU and BWU (Fuenzalida et al., 2019; Mayr et al., 2014). Furthermore, six included submersion experiments ranging from 2 h to 5 days (Liu et al., 2019; Losso et al., 2021; Mason Earles et al., 2016; Matsunaga et al., 2021; Mayr et al., 2014; Tomasella et al., 2022). Submersion is a condition stems are unlikely to experience outside of extreme flooding and as a result, possibly overestimates the contribution of BWU. Rather, fog, dew and rain likely form the dominant sources for BWU, as with FWU (Schreel & Steppe, 2020). The limited number of studies and the variability of the methods employed make it difficult to infer the contribution that BWU makes to whole plant hydration. In addition, to date, no study has identified a pathway for water movement from the outer surfaces of the bark to the inner tissues, other than permeation across the bark surface.

Combined global bark surface has an estimated area of 41 million km^2, although this is likely an underestimation as it does not take into account bark surface complexity which can add 10%–16% to bark surface area relative to a smooth surface (Van Stan et al., 2021). Unlike leaves in many species, the outer bark is an organ that is present year-round (Van Stan et al., 2021), including during drought when many species shed their leaves to reduce water loss (Wolfe et al., 2016; Wolfe, 2020). Therefore, the bark surface represents a huge area over which water uptake could occur to substantially improve hydration, especially where environmental conditions limit hydration through FWU or roots.

Mangroves are likely candidates for BWU due to limitations imposed by salinity on water uptake. Increasing salinity reduces the water potential (ψ) of the estuarine water at the roots ($\psi_{salinity}$), thereby limiting hydration as $\psi_{salinity}$ sets the upper limit for hydration achievable through the roots (Scholander et al., 1964). For example, Nguyen, Meir, Sack, et al. (2017) found that leaves of three subspecies of *Avicennia marina* would not achieve full hydration or become fully turgid from absorption of soil water alone where $\psi_{salinity}$ was −1.92 to −3.36 MPa. Therefore, to achieve hydration greater than that of $\psi_{salinity}$, FWU or BWU is required. Indeed, a diversity of pathways for FWU has been found in many species of mangrove (e.g., Bryant et al., 2021; Fuenzalida, Blacker, et al., 2022; Hayes et al., 2020; Schaepdryver et al., 2022) demonstrating widespread capacity for top-down rehydration.

Similar to FWU in mangrove leaves (Bryant et al., 2021; Coopman et al., 2021; Nguyen, Meir, Sack, et al., 2017), we hypothesise that BWU in mangroves will occur through controlled entry points, rather than passive diffusion across bark surfaces. As in leaves, control of water fluxes across bark surfaces would be essential to protect the stem tissues from hazardous effects of dehydration, and prevent toxic effects from unrestricted entry of salt that accumulates on bark surfaces due to sea-spray and periodic wetting by saline tidal water. Lenticels—pores found in the tissue of the outer bark—may provide such a controlled entry point for BWU.

Lenticels provide pathways for gas exchange between inner tissues and the atmosphere (Lendzian, 2006). Rosner and Morris (2022) speculated that lenticels may be involved in BWU; however, it is unknown if a trade-off between their gas exchange function and water uptake is possible, as has been found in stomata for FWU (Binks et al., 2020; Burkhardt et al., 2012; Eichert et al., 2008; Guzmán-Delgado et al., 2021; Vesala et al., 2017). Indeed, the wax covering of the inner surface of the lenticel is thought to prevent liquid water from entering the lenticel, as gas exchange must be maintained during rain (Lendzian, 2006; Rosner & Morris, 2022). Nevertheless, lenticels form a channel for exchange between inner stem tissues and the atmosphere, and so we hypothesise that lenticels facilitate BWU in mangroves due to the requirement to regulate water uptake.

BWU is driven by the ψ difference across the bark surface, requiring the water that accumulates on a bark surface to have a less negative ψ than that within the stem. As per Ohm's law analogy (van den Honert, 1948), rates of water uptake across leaf or bark surfaces depend on the strength of the ψ gradient and the resistance along the gradient. For example, refilling of embolised vessels following BWU was greatest in mildly dehydrated branches of *Salix matsudana*, and when exposed to light (Liu et al., 2019). The authors hypothesised that corticular photosynthesis under light promoted nonstructural carbohydrate accumulation, creating a stronger ψ gradient for water movement through the bark comparable with ψ gradients generated with mild dehydration. However, embolism refilling decreased under severely dehydrated conditions (Liu et al., 2019) likely due to decreased hydraulic conductance through living cells in the stem with increasing dehydration, as in leaves (Scoffoni & Sack, 2017; Trifiló et al., 2016). Therefore, BWU may increase in response to greater ψ gradients and light, but decline when ψ in the stem becomes more negative than the turgor loss point, with water stress and darkness inhibiting water uptake.

Last, as daytime transpiration increases demand for water at the leaves, stems shrink, and as stomata close and the tree rehydrates, stems swell. The source of this 'pulse' has been identified as the discharge and recharge of water storage from elastic living tissues (Nehemy et al., 2022; Sevanto et al., 2011; Steppe et al., 2012; Treydte et al., 2021; Zweifel et al., 2001) that maintain stem hydraulic function, as the water released from storage tissue buffers development of tension in xylem conduits during rapid transpiration (Meinzer et al., 2008; Pfautsch, Hölttä, et al., 2015). It is hypothesised here that BWU may play an important role in the recharging of living stem water storage tissues such as the cortex, and hence may facilitate stem swelling.

The present study investigated BWU in stems of *Avicennia marina*. *A. marina* is the most widely distributed mangrove globally (Morrisey et al., 2010), capable of tolerating hypersaline conditions up to twice that of seawater (Reef et al., 2012). FWU in *A. marina* demonstrates capacity for top-down rehydration (Coopman et al., 2021; Fuenzalida, Blacker, et al., 2022; Nguyen, Meir, Sack, et al., 2017; Schreel et al., 2019; Steppe et al., 2018); however, capacity for BWU remains untested. We tested the following hypotheses:

1. BWU occurs primarily through lenticels on the outer bark surface.
2. BWU will increase as stem ψ decreases reflecting greater ψ gradients for uptake, until turgor loss where uptake will decrease due to decreased conductance.
3. BWU will be greater in light than dark conditions.
4. BWU will be sufficient to cause swelling of water storage tissues in the stem, as measured using X-ray microcomputed tomography.

2 | MATERIALS AND METHODS

2.1 | Species

All experiments were conducted on *Avicennia marina* subsp. *australasica* (Walp.) J.Everett., saplings (Supporting Information: Figure S1), 30–50 cm tall. Saplings were raised from propagules collected in 2019 from the Clyde River in New South Wales, Australia, and grown hydroponically in solutions of 50% seawater amended with nutrients under glasshouse conditions at the Australian National University, as described by Fuenzalida, Binks, et al. (2022).

2.2 | Common experimental features

2.2.1 | Plant material

For all experiments, saplings harvested from the glasshouse were cut at the base of the stem above root growth. The severed shoots were placed in black plastic bags to reduce water loss during transportation to the lab. The target stem section used for all BWU experiments was the bottom most length of stem (6–9 cm in length) with the most mature bark (hereafter referred to as 'stem', Supporting Information: Figure S1) cut from each shoot. Stems had an average diameter of 8 mm.

2.2.2 | Stem water potential

Where indicated in the experimental particulars below, initial stem water potential was measured. Severed shoots were placed in black bags for 30 min to allow equilibration of ψ across the stem and attached leaves. The youngest, healthy, fully expanded leaf from each shoot was cut at the petiole and measured for ψ using a Scholander pressure chamber (Pressure chamber model 1050D; PMS Instrument).

2.2.3 | Sealing of stem cut ends

Before each experiment, the stem cut ends were sealed to prevent water entry. A coat of petroleum jelly (Vaseline) was smeared over the cut ends and extended 5 mm along the stem length to create a barrier cuff. Cut ends were then wrapped tightly with Parafilm. The point at which the Parafilm ended and the exposed bark began was sealed with orthodontic wax. The efficacy of the seal on the cut ends of the stem was validated using disodium fluorescein (see Section 2.3 described below). The seal was found to be effective (Supporting Information: Figure S2) and was therefore used in all subsequent experiments.

2.2.4 | Stem characteristics

To establish baseline stem characteristics, stem diameter, total stem length and length of exposed bark surface between each Parafilm seal was measured. Stem surface area and volume were then calculated assuming a cylindrical shape. For measurement of stem dry mass (DM), Parafilm seals were removed at the completion of each experiment and the stems were oven-dried at 60°C (LABEC Laboratory Equipment, Pty. Ltd.) for 4 days until constant mass was achieved. These stem characteristics were later used to determine stem water content (WC, g) per initial stem surface area, stem volume and stem DM.

2.2.5 | Mass based measurement of BWU

Stems were weighed (XP 205 Metter Toledo balance; Mettler-Toledo Ltd.) before and after sealing of stem cut ends (Section 2.2.3) for initial stem mass before BWU. Stems were then placed in individual wetting chambers. Wetting chambers were 50 mL FALCON Conical Centrifuge Tubes with stiff plastic mesh to hold the stem above any liquid water, and a damp tissue in the bottom of the tube to increase humidity. Stems inside wetting chambers were sprayed liberally with tap water from a nasal spray atomiser to replicate small water droplets from rain, fog or dew, and sealed with lids. Stem mass was recorded at 0.5, 1, 2, 4, 6, 9 and 12 h of BWU. Water films were visible on bark surfaces throughout the measuring period. Before mass was recorded at each interval, stems were patted dry with dry paper towel. Parafilm seals were inspected on each individual to ensure a strong seal remained. Following each measurement, stems were again sprayed with water to ensure liquid water was present on the surface of the stem and wetting chamber lids closed. Wetting chambers were placed horizontally in a growth chamber (TRIL-1175-SD-1SL Thermoline Scientific Growth Chamber; Thermoline Scientific Equipment Pty. Ltd.) at 22.1°C under full spectrum grow lights for the duration of the experiments.

2.3 | Pathways for BWU

Fluorescence microscopy was used to identify pathways for BWU in *A. marina* using the symplastic tracer dye disodium fluorescein (fluorescein; Moon et al., 1986). Three *A. marina* stems (Supporting Information: Figure S1) were cut into three segments, each approximately 3 cm long. Stem cut ends were sealed (Section 2.2.3), and the segments from each

sapling were assigned to one of three incubation periods (0.5, 1 and 2 h). Segments were sprayed with 1% w/v fluorescein from a nasal spray atomiser to mimic the fine droplets from fog, rain and dew, and incubated in a Petri dish under laboratory bench conditions (21°C). Thus, measurements were made after incubation with fluorescein for three different time periods for each stem, and replicated in three individuals.

Before analysis stems were blotted dry, and the Parafilm seals were removed. The bark of each segment was observed under a Zeiss Axiostar Plus epifluorescence microscope with filter cube Dapi/Fitc/Tritc (Chroma 96000; Chroma) and illuminated with a CoolLED PE300-W at the lowest blue light intensity. RAW format images were captured using the Halide Mark II Pro Camera app on an iPhone XR (iOS15.6.1) mounted on the microscope eyepiece. The purpose was both to identify bark surface features that could act as entry points for fluorescein, and to validate the efficacy of the seal on the cut ends of the stem (see Section 2.2.3, Supporting Information: Figure S2).

The central portion of each segment was carefully rinsed with water and patted dry. Transverse sections 100 µm and 200 µm thick were cut on a sledge microtome G.S.L.1 (S. Lucchinetti; Schenkung Dapples) and placed dry on a slide with a coverslip on top as oil was found to diminish the fluorescein signal during preliminary testing. Sections were observed under a Zeiss Axiostar Plus epifluorescence microscope as described above, under both fluorescence and brightfield. This procedure was repeated for three additional stems, each cut into two segments. Each segment from each stem was assigned to either 4 or 6 h of incubation.

Three transverse slices from each treated stem segment were analysed using Fiji imaging software (Schindelin et al., 2012) for area (mm^2) of each tissue layer, area of the stem with fluorescein, percent of stem area with fluorescein, and penetration depth of fluorescein from bark to pith. Tissue layers were defined as per Figure 1. Where an entry point in the bark could be identified, its characteristics were

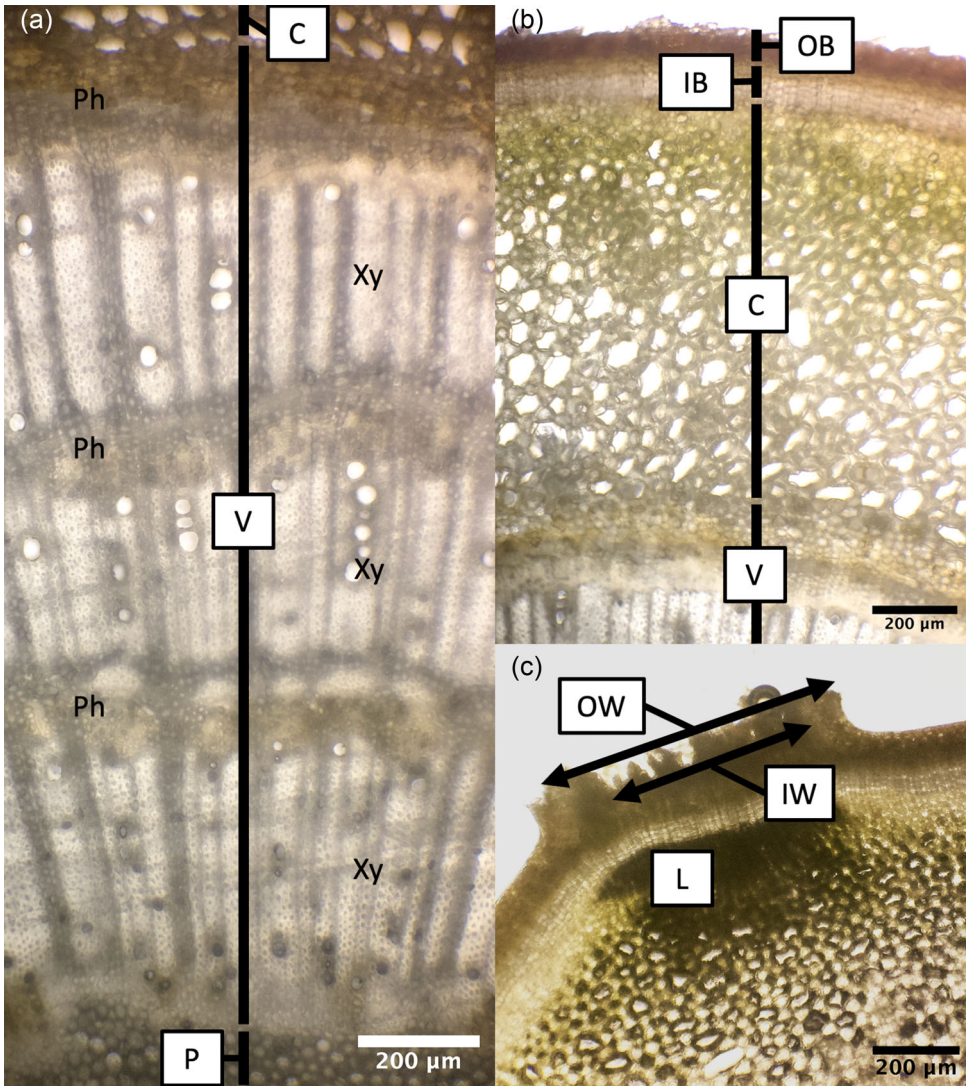

FIGURE 1 Fresh transverse stem sections of *Avicennia marina* subsp. *australasica* showing definition of tissue layers in the vascular tissue (a), cortex and bark (b), and lenticel (c). C, cortex; IB, inner bark; IW, inner width; L, lenticel; OB, outer bark; OW, outer width; P, pith; Ph, phloem; V, vascular; Xy, xylem.

measured, including area, width and the penetration depth of fluorescein directly under the bark feature.

Fluorescein was identified in the inner stem tissues in all samples from all individuals following bark exposure. However, preliminary analysis revealed substantially less visible fluorescein following 4 and 6 h of exposure, compared with exposure of 2 h or less. It is unlikely that stems of *A. marina* took up less fluorescein over time. Rather we hypothesise that fluorescein was transported away from the location of uptake and/or was transported into vacuoles where the more acidic pH quenched the fluorescence signal (Doughty, 2010; Oparka, 1991). For this reason, only fluorescein uptake results from 0.5, 1 and 2 h of exposure are presented in the Results below. Results from all exposure treatments can be found in the supporting information (Supporting Information: Figures S3 and S4).

To capture greater detail of fluorescein location within the stem tissue of *A. marina*, two additional individuals were collected from the greenhouse. Stems were treated as above for 0.5, 1 and 2 h of fluorescein exposure. Images were acquired at the Australian National University (ANU) Centre for Advanced Microscopy using ZEN 2.6 on a Zeiss Observer.Z1 with a 5 × 0.16 NA lens and an Axiocam 506 monochrome camera. Zeiss filter sets 43HE, 38HE and 49 in conjunction with a Colibri.2 LED light source were used for red autofluorescence, green (Fluorescein) and blue autofluorescence channels, respectively. A transmitted light image of the same region was also acquired.

2.4 | Stem anatomy

Transverse slices 100 µm and 200 µm thick from five *A. marina* stems (Section 2.2.1) were observed under a Zeiss Axiostar Plus epifluorescence microscope as described above (see Section 2.3). Images were taken under brightfield to characterise *A. marina* stem anatomy, and under blue light to compare fluorescence signals in stems with and without fluorescein exposure. Two transverse slices for each individual were analysed using Fiji imaging software (Schindelin et al., 2012) and averaged to capture variation within the stem for stem tissue layer thickness and area. Tissue layers were defined as per Figure 1. Vessel size and density were measured in an area of 1 mm^2 within the vascular tissue. Results are presented in the supporting information (Supporting Information: Tables S1 and S2).

2.5 | Effect of dehydration on BWU

Twenty *A. marina* saplings were randomly assigned to one of four dehydration treatments: no dehydration (equilibration with $\psi_{salinity}$), 0.5 h of dehydration, 1 h of dehydration and dehydration to turgor loss. Each sapling was loosely wrapped with damp paper towel and clingfilm, and covered with a paper bag overnight to limit transpiration and bring the plants to approximate equilibration with root water (50% seawater, −1.2 MPa) overnight. The following morning, each sapling was uncovered and cut at the base of the stem.

The severed shoots (Supporting Information: Figure S1) assigned to no dehydration were immediately equilibrated for measurement of ψ as in Section 2.2.2, while shoots assigned to dehydration treatments of 0.5, 1 and dehydration to turgor loss were placed inside a growth chamber (TRIL-1175-SD-1SL Thermoline Scientific Growth Chamber; Thermoline Scientific Equipment Pty. Ltd.) at 22.1°C under full spectrum grow lights to dehydrate for their allotted time. Shoots assigned to dehydration to turgor loss were incrementally dehydrated and measured for ψ (see Section 2.2.2) in 1–1.5 h intervals for a total of 4.5 h until change in ψ had slowed, indicating the turgor loss point has been reached (Nguyen, Meir, Wolfe, et al., 2017). Henceforth, this treatment will be referred to as 4.5 h of dehydration.

The BWU stem was cut from the shoot and ends were sealed (see Section 2.2.3). Baseline stem characteristics were recorded as described in Section 2.2.4. Stems were measured for BWU as described in Section 2.2.5.

2.6 | Effect of light exposure on BWU

In the early evening, 15 *A. marina* saplings were randomly assigned to one of light, dark or bare stem treatments, wrapped with damp paper towel and clingfilm for equilibration with root water (50% seawater, −1.2 MPa), and covered by a black plastic bag and a thick paper bag to prevent light exposure before the treatment. The following morning, paper bags were removed and shoots were cut while remaining covered by the black plastic bags.

The following procedure was carried out in low light to prevent light exposure outside of the assigned treatment during stem preparation and measurement. All shoots were equilibrated, and measured for ψ as in Section 2.2.2. The BWU stem was cut from the shoot and ends of stems assigned to light and dark treatments were sealed (see Section 2.2.3). The stems assigned to the bare stem treatment were left unsealed to measure the rate of water uptake when vascular tissue was exposed at the cut ends (Supporting Information: Figure S5). Baseline stem characteristics were recorded as described in Section 2.2.4. The five wetting chambers assigned to the dark treatment were wrapped with foil to ensure no light could enter, wetting chambers assigned to light and bare stem treatments were left uncovered. Stems were measured for BWU as described in Section 2.2.5.

2.7 | X-ray micro-computed tomography (XMCT) stem swelling following BWU

XMCT was used to discern changes in stem dimensions and the sources of those changes in response to BWU. One *A. marina* sapling with straight, mature stem <10 mm in diameter was equilibrated overnight with root water as described in Section 2.5. The BWU stem was cut from the shoot and ends were sealed (see Section 2.2.3). Baseline stem characteristics were recorded as described in Section 2.2.4. Two additional replicate stems were selected and

treated as above, except that the stems were left uncovered overnight and dehydrated in a growth chamber for 1 h before the experiment. This dehydration step to reduce turgor pressure was done to facilitate a greater magnitude of expansion upon rehydration for visualisation, assuming a maximum extent of swelling with full turgor.

Each stem was wrapped tightly with dry paper towel and placed into a 10 mm diameter glass tube sealed with a thin silicone bung through which a needle was inserted for later application of water. Stems were scanned at the National Laboratory for X-ray Micro Computed Tomography (CTLab, ANU), using a HeliScan MicroCT system with an optimized space-filling trajectory (Kingston et al., 2018) to yield sharp images (Latham et al., 2008; Myers et al., 2011). Full spectrum LED grow lights (Urban Plant Growers) were fitted inside the system and remained on for the duration of the experiments. XMCT scans were acquired at an energy of 60 kV and a current of 60 μA, which allowed repetitive scans on the same stem without causing visible damage. Two initial scans were taken before the addition of water, both using a space-filling helical-scanning trajectory (Varslot et al., 2011) comprising 1.94 revolutions; the first was a 70-min high-definition high-fidelity scan (with 2880 projections per revolution, 3032 × 3032 pixels and 0.5 s exposure time per projection); the second was a faster, 17-min lower-definition scan (1440 projections per revolution, 1516 × 1516 binned pixels and 0.18 s exposure time per projection).

Using a syringe, 1.5 mL of tap water was added to saturate paper towel around the stem. For the following 2 h, scans were taken using the lower-definition fast scan parameters described above to account for any rapid swelling. The stem was then imaged using previously described high-definition scan parameters for 12 h with a final scan made at 24-h post addition of water. Stems were removed, patted dry and weighed. Anatomical images were taken as described above (see Section 2.3). All stem sections were collected and oven-dried for stem DM (see Section 2.2.4). Analysis revealed no rapid changes occurred within the first 2 h, so repeat experiments used the above-described high-definition high-fidelity scan parameters.

Reconstructed tomograms had a field of view of 10.4 × 10.4 × 9.1 mm, with high-definition data having dimensions of c. 2480 × 2480 × 2160 voxels with a voxel size of c. 4.2 μm, and lower resolution data having dimensions of c. 1240 × 1240 × 1080 voxels with a voxel size of c. 8.5 μm. Details about the reconstruction process can be found in Kingston et al. (2018). Three image slices from the same points in the stem were isolated dry and following 24 h of BWU. Measurements were made on each of these slices using Fiji image analysis software (Schindelin et al., 2012). Tissue layers were defined as per Figure 1; however, outer and inner bark were indistinguishable and so were measured collectively as 'bark'. Radius was measured from the pith to three identical points around the stem diameter dry and following BWU within each slice to control for variation around the stem circumference and uneven swelling of stem tissues. Lenticels were observed to swell considerably in response to BWU. To isolate swelling of stem tissue layers in response to BWU from changes in the stem as a result of lenticel swelling, tissue radius measurements were made on areas of the slice where no lenticels were present. To characterise lenticel swelling effects, tissue radius measurements were made from the pith to the centre of each lenticel. Area, height, pore inner width and pore outer width were measured for each lenticel dry and following 24 h of BWU. The threshold tool in Adobe Photoshop 2022 was used to measure changes to gas spaces within the stem sections.

2.8 | Statistical analysis

Statistical analyses were performed using the R statistical software package R Core Team, 2023 version 4.3.1).

A linear model with treatment as a fixed effect was used to test the effect of dehydration (Table 1>) and light exposure (Figure 5) on BWU. The Anova() function in the *car* R package (Fox & Weisberg, 2019) was used to assess the significance of main effects at the $p < 0.05$ level.

Changes to stem tissues dry and following 24 h of BWU from XMCT experiments (Table 2) were assessed with a linear mixed effects model with treatment as a fixed effect and random intercepts for each individual, slice analysed and measurement point within the slice using the lmer() function in the *lmerTest* R package (Kuznetsova et al., 2017). The anova() function was used to assess the significance of main effects and interactions at the $p < 0.05$ level.

Model fit was assessed through a number of diagnostic tests, including diagnostic residual plots and the Shapiro–Wilk test, and where necessary dependent variables were log-transformed to improve model fit. Model estimated marginal means, standard error (SE) and mean difference were produced using the *emmeans* R package (Lenth, 2020). Figures were produced using the package *ggplot2* (Wickham, 2016).

3 | RESULTS

3.1 | Pathways for BWU

Lenticels on the bark surface were identified as a pathway for fluorescein entry from outer bark to inner stem tissues (Figure 2). In every stem slice analysed where a lenticel was visible, fluorescein was found in the inner stem tissues. Furthermore, fluorescein was consistently observed in the tissue of the lenticel, in the cells connecting the lenticel structure to the cortex through the inner bark (Figure 2d,e), and in the cortex directly underneath the lenticels (Figure 2g,h). While other pathways for fluorescein entry through the bark cannot be ruled out, lenticels were the only structure that could be identified as a pathway. Within the vascular tissue, fluorescein could be identified in the phloem layers, appearing to move further into the stem towards the pith through parenchyma ray cells, and into vessel and surrounding fibre tissues after just half an hour of exposure (Figure 2). Images of stems without fluorescein revealed that the bright green fluorescence signal associated with fluorescein could be clearly distinguished from stem

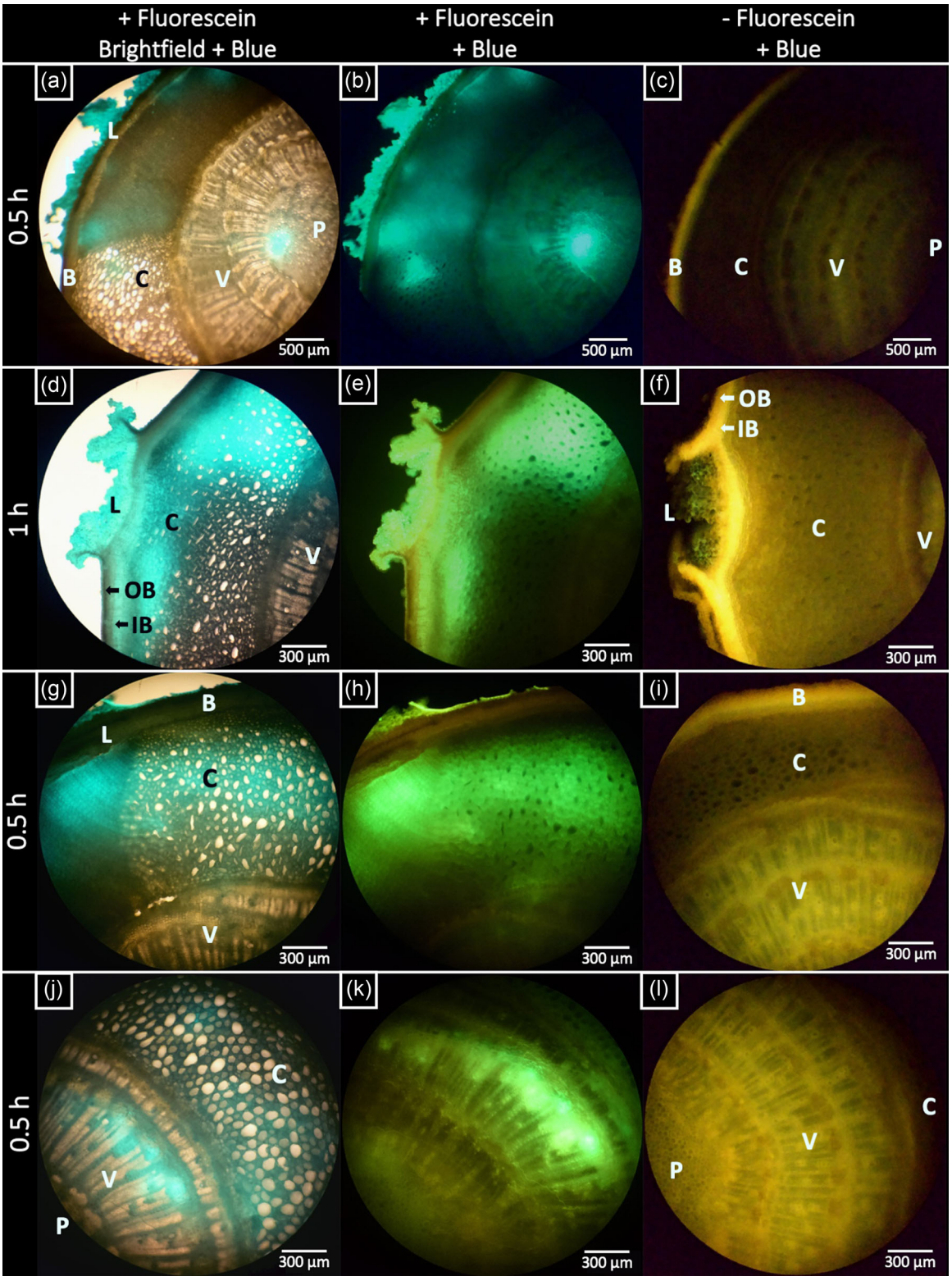

FIGURE 2 (See caption on next page).

autofluorescence even when multiple channels of excitation were included to illuminate autofluorescence (Figures 2 and 3).

On average (±SE) across 0.5–2 h of bark exposure, the maximum penetration of fluorescein from inner bark towards the pith was 2.2 mm (±0.21), while the average penetration of fluorescein was 1.3 mm (±0.15). The average radius of *A. marina* stems measured for fluorescein uptake was 3.2 mm, meaning that fluorescein penetrated approximately 69% of the depth of the stem from bark to pith.

On average, the percent of the total stem area occupied by fluorescein was greatest after 1 h, with dye visible in 21.1% of the stem area; however, 13.4% of the total stem area was occupied by fluorescein after just 0.5 h of bark exposure (Figure 4). After 1 h, the cortex tissue had the greatest amount of fluorescein visible, with 38.6% of the area occupied by fluorescein, followed by the pith area with 19.5%, and the phloem area with 12.5% occupied by fluorescein. Fluorescein was visible in the xylem tissue (Figures 2 and 3); however, substantially less fluorescein was visible in xylem (2.9%) compared with other tissues. Fluorescein was visible in the inner bark tissue only where dye had entered through a lenticel.

3.2 | Effect of dehydration on BWU

Stems of *A. marina* were exposed to one of four dehydration treatments inducing increasingly lower initial stem ψ to measure the effect of dehydration on the subsequent amount and rates of BWU.

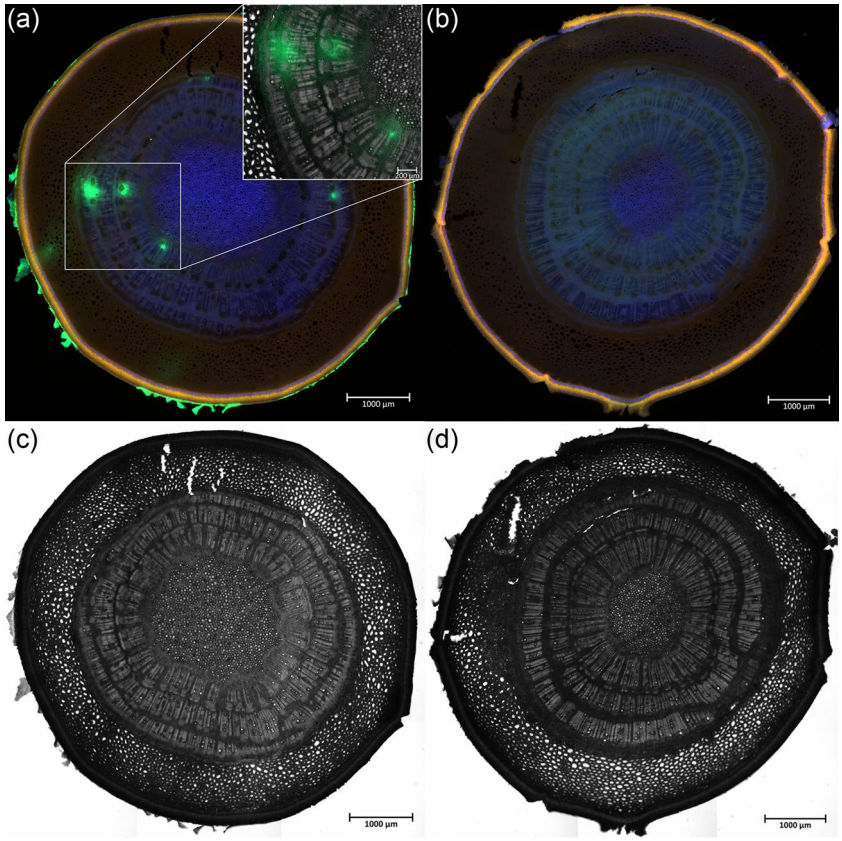

FIGURE 3 Fresh transverse sections of *Avicennia marina* subsp. *australasica* stems with (a,c) and without (b,d) bark exposure to disodium fluorescein taken with a Zeiss Observer.Z1 with red, green and blue light excitation and a brightfield channel. Images of stem sections are shown as pairs where the images on the top row show the combined red, green and blue fluorescent emission (a,b), while images on the bottom row are the brightfield images of the same section to show details of stem structure (c,d). Both samples were imaged under identical conditions. A region of interest was identified from image (a) where fluorescein fluorescence was visible in the vascular tissue of the stem. This region was reimaged at lower exposure to reduce camera saturation and provide greater detail of fluorescein location within the vascular tissue (a). A gamma adjustment of 0.45 was applied to this image to allow better visualisation of the pathway for fluorescein movement through the vascular tissue. A version of this image where all fluorescence channels are displayed can be viewed in the supporting information (Supporting Information: Figure S6). [Color figure can be viewed at wileyonlinelibrary.com]

FIGURE 2 Fresh transverse sections of *Avicennia marina* subsp. *australasica* stem lenticels and main tissues of interest showing the pathway of bark water uptake and water movement within stems as indicated by fluorescence emitted by disodium fluorescein, following its application to bark surfaces. Each sample is shown in a pair of exemplary images with the left image taken under epi-fluorescent brightfield illumination plus blue light excitation to show the location of the green fluorescein fluorescence signal within the stem structure (a,d,g,j), and the central image taken under epi-fluorescent illumination with blue light excitation to show distribution of fluorescein within the stem (b,e,h,k). An additional image is included on the right of each pair showing a section of stem of similar orientation and structure from separate hydrated samples without disodium fluorescein taken under epi-fluorescent illumination with blue light excitation (c,f,i,l). C, cortex; B, bark; IB, inner bark; L, lenticel; OB, outer bark; P, pith; V, vascular. (a,b) Transverse stem section showing fluorescein in a lenticel and the adjacent cortex, vascular and pith tissue. (d,e) Transverse stem section showing presence of fluorescein extending from the outer lenticel tissue, through the lenticel, into inner bark and cortex tissue. (g,h) Transverse stem section showing transportation of fluorescein applied to bark surfaces through a mature lenticel, through rays of photosynthetic cortex tissue, and into surrounding tissue. (j,k) Transverse stem section showing transportation of fluorescein applied to bark surfaces into vascular tissue, visible in phloem, parenchyma ray cells and vessels—note that this pair are from the same stem but the images are shifted to different positions to cover the transition from the cortex into the xylem. [Color figure can be viewed at wileyonlinelibrary.com]

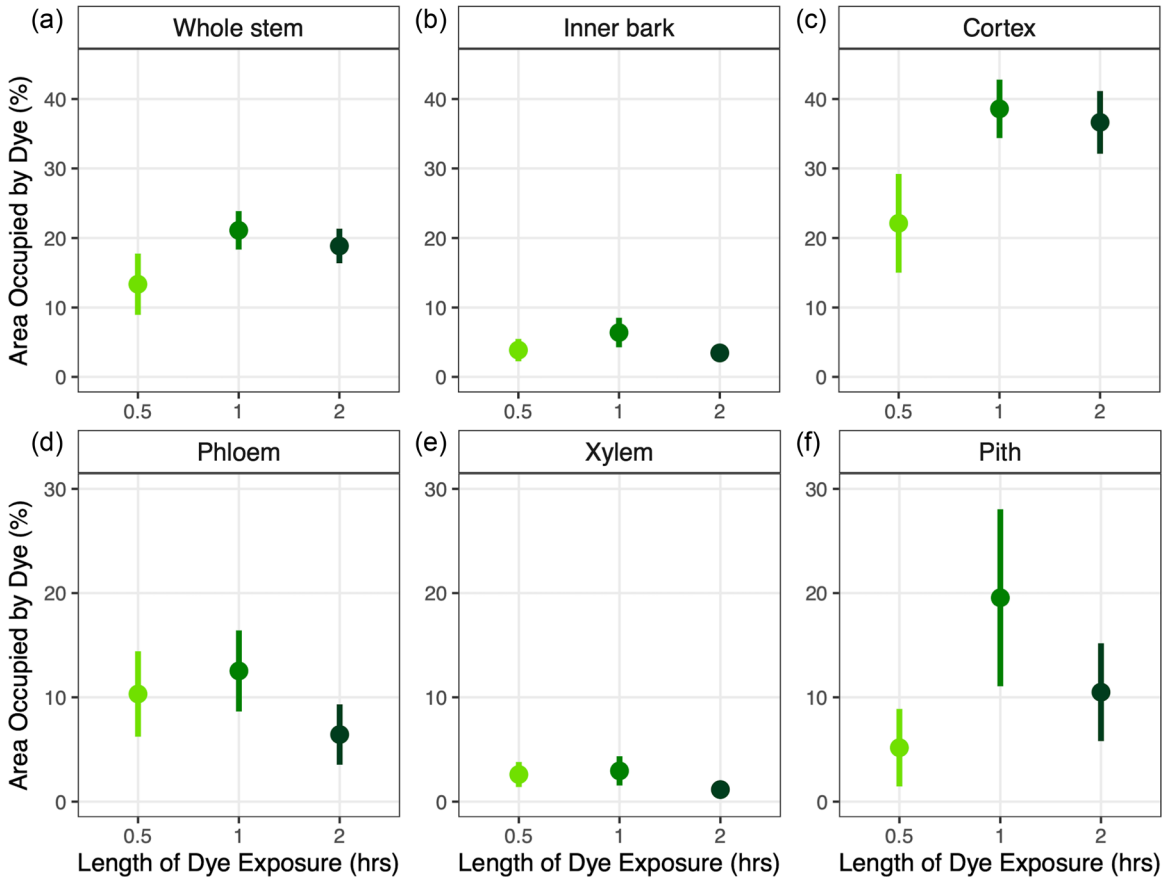

FIGURE 4 Percent of tissue area exhibiting fluorescence emitted by the dye disodium fluorescein visible in fresh transverse sections of *Avicennia marina* subsp. *australasica* stems following incubation of stem surfaces in dye solution for 0.5, 1 or 2 h (light green, green and dark green, respectively). (a) whole stem, (b) inner bark, (c) cortex, (d) phloem, (e) xylem, and (f) pith. Values are observed means ± SE, $n = 3$. [Color figure can be viewed at wileyonlinelibrary.com]

TABLE 1 Bark water uptake (BWU) characteristics in stems of *Avicennia marina* subsp. *australasica* following bench drying for different durations to produce a range of initial water potentials.

Parameter	Unit	Estimated marginal mean ± SE $n = 5$ Dehydration exposure (hours) 0	0.5	1	4.5	*p* Value
Initial water potential	MPa	−1.36 ± 0.12	−3.45 ± 0.12	−4.15 ± 0.12	−4.74 ± 0.12	<0.0001
Total increase in WC	g gDM^{-1}	0.037 ± 0.006	0.035 ± 0.005	0.032 ± 0.005	0.035 ± 0.005	0.952
	g m^{-2}	27.9 ± 4.7	26.5 ± 4.5	35.1 ± 5.9	36.1 ± 6.1	0.474
	g m^{-3}	14076 ± 2630	16276 ± 3041	21392 ± 3997	20695 ± 3866	0.362
Increase in WC (Relative to initial WC)	%	3.05 ± 0.49	2.76 ± 0.44	2.82 ± 0.45	3.25 ± 0.52	0.881

Note: All values for BWU are based on total changes in stem WC over a 12-h period with normalisations based on stem dry mass, initial stem surface area, or volume. Values are estimated marginal means ± SE, $n = 5$, from a linear model with treatment as a fixed effect. *p* Values represent significance of differences between treatment effects. Data for all parameters excluding initial water potential were log-transformed for analyses to account for nonnormality of model residuals. Corresponding observed means ± SE are given in Supporting Information: Table S3 and results from associated ANOVAs in Supporting Information: Table S4.

Abbreviation: WC, water content.

Stems assigned to no dehydration (0 h) had an average ψ of −1.36 MPa confirming approximate equilibration with the hydroponic culture solution of −1.2 MPa (50% seawater). The group receiving the 4.5 h dehydration treatment had an average ψ of −4.74 MPa (Table 1), confirming dehydration beyond the turgor loss point was achieved, comparable with the turgor loss point of −4.5 MPa (± 0.1) recorded in the source population growing at 80% seawater with a ψ of −1.92 MPa (Nguyen, Meir, Sack, et al., 2017). ψ of the treatment

groups were significantly different ($p < 0.0001$) indicating the efficacy of the dehydration exposure treatment. However, variation in the initial dehydration state over the range from −1.36 to −4.74 MPa did not significantly impact the increase in WC following 12 h of BWU (Table 1), or the rate of uptake at any point over the 12 h of measurement (Supporting Information: Table S4 and Figure S7).

3.3 | Effect of light exposure on rates of BWU

Stems of *A. marina* were measured for BWU under either darkness or light for 12 h. Enhancement of WC by light was weakly significant when WC was expressed per stem DM ($p = 0.054$) and volume ($p = 0.056$), suggesting a trend towards increased BWU under light conditions (Figure 5). On average, stems under light conditions increased their WC by 1.5–2.2 times greater than stems under dark conditions, showing the greatest difference in rate of water uptake between the treatments over the first 4 h of measurement (Figure 5). The rate of uptake in stems under dark conditions increased over the first 2 h of uptake, reaching a maximum rate of uptake between 2 and 4 h of uptake. Conversely, the rate of uptake in stems under light conditions was greatest in the first half hour of uptake and decreased rapidly between 0.5 and 2 h of uptake before converging with the rate of uptake under dark conditions at 6 h of uptake.

3.4 | BWU as a source of stem swelling

Stems of *A. marina* with a mean radius of 3.05 mm (±0.09) were imaged using XMCT before exposure to water (dry) and after 24 h of BWU (Figure 6). Stem lenticels swelled in response to BWU (Figure 7), increasing their area by an average of 0.15 mm^2 (Table 2). Much of this increase in area was driven by swelling of the outer bark component with water, as indicated by an increase in light grey in the lenticel pore.

Measurement of stem radius showed that bark tissues and cortex swelled in response to BWU (Table 2) such that whole stem area increased by 0.825 mm^2 (±0.126). However, vascular tissue contracted significantly in response to BWU such that whole stem measurements did not capture the total radial increase in bark and cortex, increasing by 0.763 mm^2 (±0.067) and 0.283 mm^2 (±0.053), respectively. Figure 6 shows that swelling of the living corticular cells resulted in an expansion of the apoplastic gas spaces of the cortex, in the stem, similar to Hoberman mechanism (Hoberman, 1990) or the expansion of honeycomb paper when stretched. The XMCT images revealed widespread embolism in xylem vessels before wetting of stem surfaces, likely developed during harvesting of stem sections. No evidence of conduit refilling was found after BWU.

Increases in WC following 24 h of BWU (Table 3) were consistent with increase in WC from dehydration and light exposure experiments, where stems were only exposed to BWU for 12 h. This indicates that exposure to BWU for 24 h did not substantially increase WC beyond that achieved over 12 h. Furthermore, mean rates of WC increase following 24 h of BWU (Table 3) were comparable with the rates of uptake measured under dark conditions (Figure 5).

4 | DISCUSSION

BWU may provide a crucial source of water during drought to maintain WC and hydraulic function, and to facilitate recovery. Yet few studies have explicitly tested for BWU. We found that BWU occurred through lenticels in stems of *A. marina* via selective pathways, minimising risks of unrestricted water entry. Furthermore, stem swelling in response to BWU indicated filling of stem water storage tissues that would prevent cellular damage and buffer xylem function during dehydration.

4.1 | A novel role for lenticels as a pathway for BWU that improves stem hydration

To date, no study investigating the role of BWU has identified a pathway to facilitate water uptake. As hypothesised, we provide novel evidence that lenticels on the outer bark surface facilitate BWU of liquid water, improving stem hydration. Previous studies have suggested that lenticels act as channels for water movement. Gil et al. (2000) found that water was confined to lenticels and lenticular channels in cork cylinders soaked for 3 days, while a study on isolated periderm strips found lenticels to be far more permeable to liquid water under vacuum infiltration than the surrounding periderm (Schönherr & Ziegler, 1980). However, research into lenticel permeability has primarily focused on water vapour exit through lenticels (Lendzian, 2006), rather than entry of liquid water. Thus, it was unknown if a trade-off could exist between their primary role in stem gas exchange, and uptake of liquid water (Lendzian, 2006; Rosner & Morris, 2022). Here, we demonstrated that intact lenticels facilitate liquid water movement from the bark surface to the inner stem (Figure 2).

Lenticels varied in size and shape, but shared a common feature that integrated them into the fabric of stem structure: columns of cells arrayed radially from the base of the lenticel, fanning into the cortex and linking across the cortex to the vascular cylinder. These radial columns were similar to the phelloderm structure of lenticels in the mangroves *Avicennia germinans* and *Rhizophora mangle* (Yáñez-Espinosa & Angeles, 2022). It is likely that these radial columns of cells facilitate movement of water from the lenticel pore into the stem, as the distribution of fluorescein indicates their role in symplastic and transmembrane distribution of liquid water from lenticels to underlying corticular and vascular tissues (Figure 2). While we cannot rule out other pathways for BWU, anatomical analyses, patterns of fluorescein uptake (Figure 2) and XMCT imaging (Figure 6) provide compelling evidence that lenticels are the primary pathway for BWU in *A. marina*.

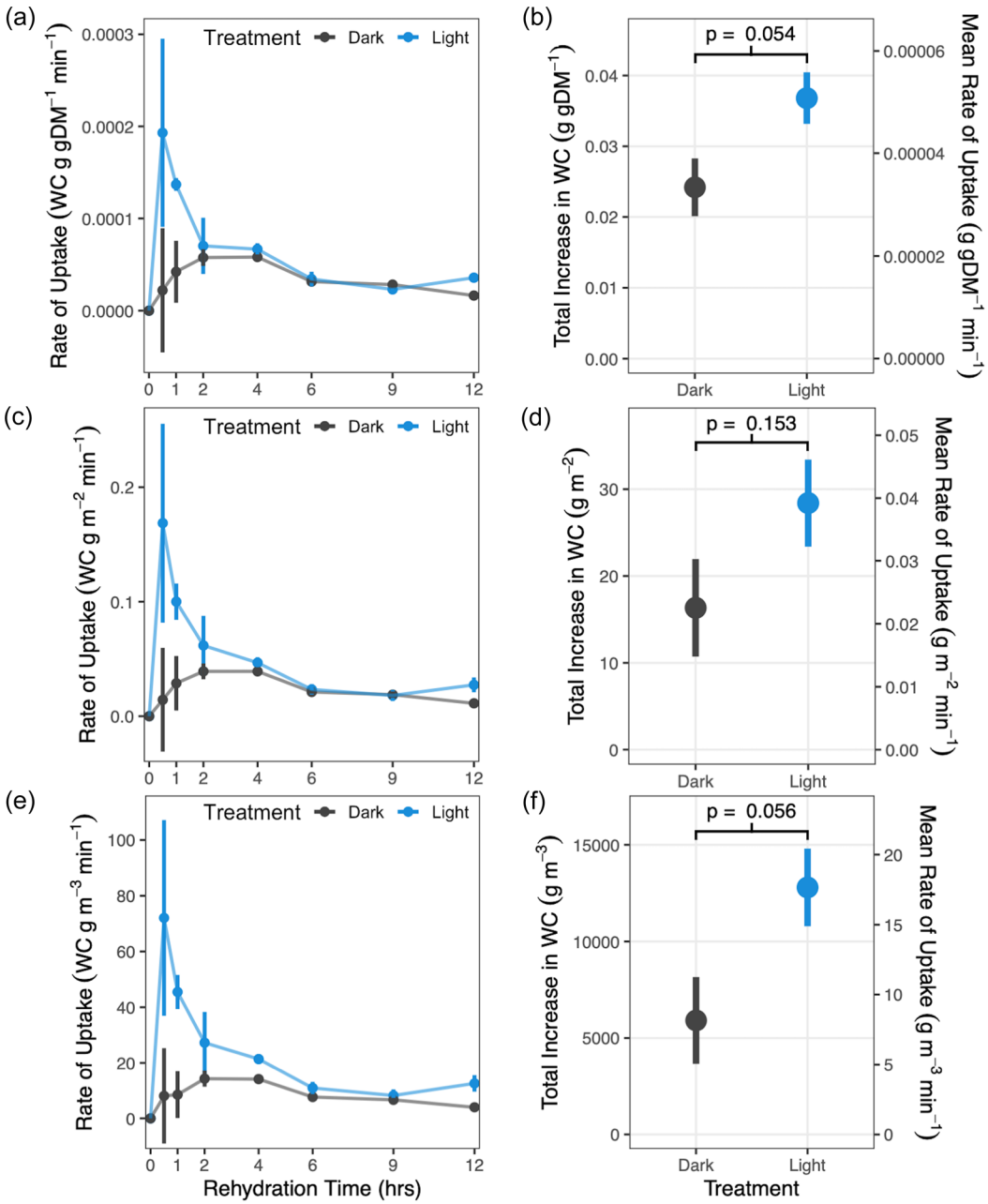

FIGURE 5 Characteristics of bark water uptake in stems of *Avicennia marina* subsp. *australasica* that were rehydrated through bark water uptake for 12 h under either dark (grey) or light (blue) conditions. Panels to the left give mean rate of uptake in water content (WC) ± SE at each rehydration time for (a) WC per dry mass (DM) per minute, (c) WC per initial stem surface area per minute and (e) WC per initial stem volume per minute. Panels to the right give estimated marginal means ± SE from a linear model with treatment as a fixed effect for (b) total increase in WC per DM, (d) total increase in WC per initial stem surface area and (f) total increase in WC per initial stem volume. Note the *y*-axis showing total increase in WC (right) is mirrored by the corresponding mean rate of water uptake (left). Light treatment $n = 5$; however, dark treatment $n = 4$ as one individual was excluded from analyses due to concerns over the security of the seal over the cut ends of the stem. *p* Values shown between the treatments represent significance of treatment effects. Corresponding observed means ± SE are given in Supporting Information: Table S5 and results from associated ANOVAs in Supporting Information: Table S6. [Color figure can be viewed at wileyonlinelibrary.com]

4.2 | Maintenance of rates of water entry minimise risk of unrestricted water entry

Dehydration did not significantly affect the average rate of BWU nor the extent of hydration, contrary to our hypothesis (Table 1). In other words, BWU did not significantly increase in response to a stronger ψ gradient driving inward water movement, nor did BWU significantly decrease due to decreased conductance as dehydration increased. Fuenzalida et al. (2019) found that recovery of leaf hydraulic conductance through shoot surface water uptake in *A. marina* was not affected by initial dehydration status, despite a decline in total uptake when shoots of were dehydrated to an initial

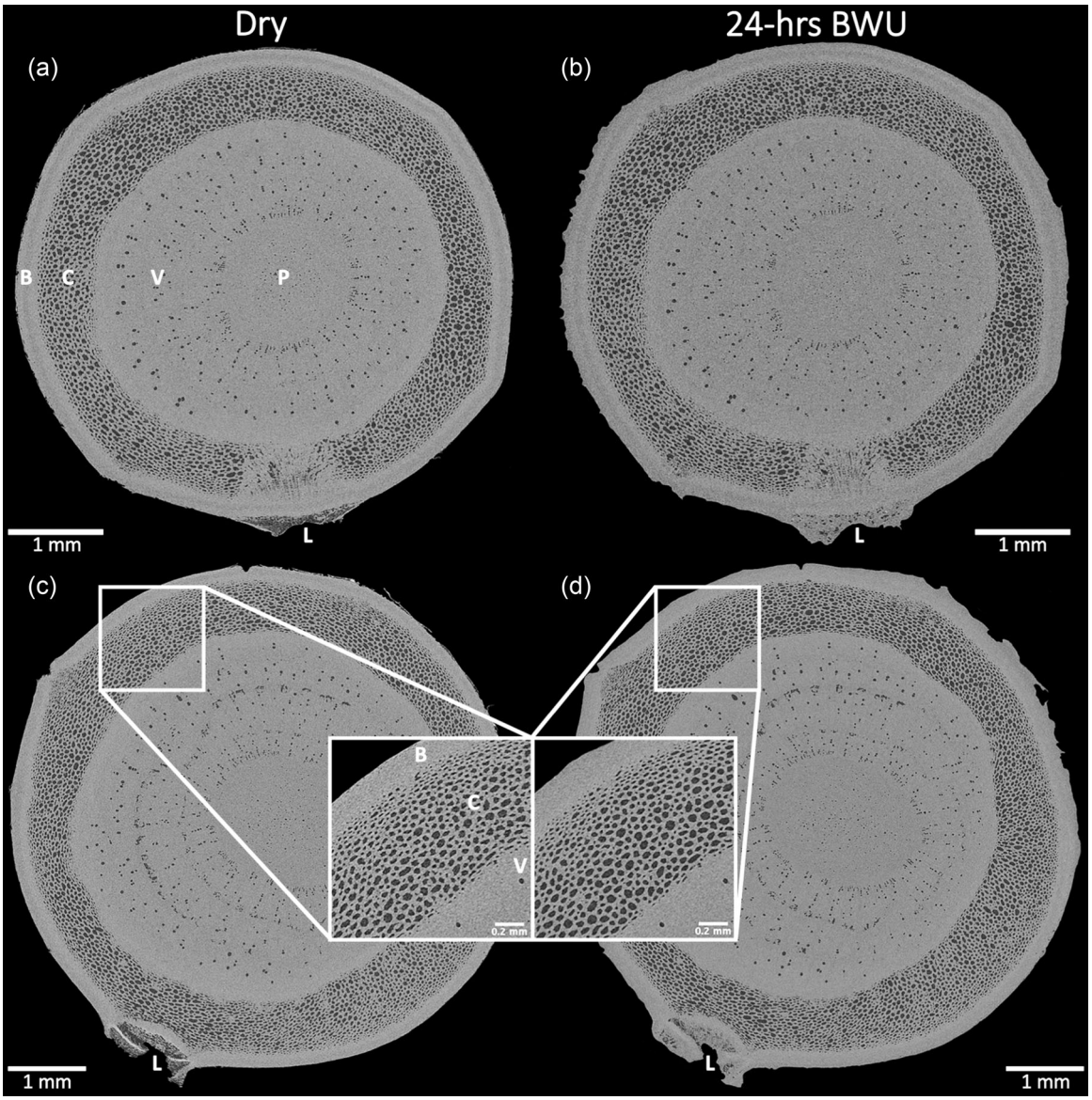

FIGURE 6 Transverse XMCT sections of *Avicennia marina* subsp. *australasica* stems showing tissues dry and following 24 h of bark water uptake (24-h BWU). Each sample is shown in a pair of images dry (a,c) and following 24-h BWU (b,d) BWU. Each image pair (a,b) and (c,d) was taken from a separate stem. A region of interest was identified from pairs c and d showing expansion of cortex tissue after BWU. Dark grey in the stem indicates gas spaces while light grey represents solid tissue and water. B, bark; C, cortex; L, lenticel; P, pith; V, vascular.

water potential of −4.9 MPa. The authors found that permeability of the leaf surface was the greatest determinant of shoot surface water uptake, not the hydraulic conductance of the mesophyll. Here, a variable resistor to water entry would be required to account for similar water uptake with variation in both the ψ gradient and conductance, thereby minimising the risk of unrestricted water entry. Therefore, permeability of lenticels may be a stronger determinant of BWU than internal conductance.

Lenticels facilitate controlled gas exchange (Lendzian, 2006; Rosner & Morris, 2022), while the periderm inhibits water loss from the stem through a combination of suberin and waxes, believed to be analogous to the epidermis and cuticle in leaves (Graça, 2015; Lendzian, 2006). By channelling BWU and gas exchange through the lenticels, the periderm can have low permeability, thus reducing water loss while still facilitating water uptake. However, even where BWU is channelled through the lenticel, in saline mangrove environments where stems may be periodically exposed to saline water, unrestricted water entry would result in movement of solutes (Serra et al., 2022), including toxic accumulation of salts within the stem tissue. Channelling BWU through lenticels in *A. marina* would reduce water lost through bark, decreasing the risk of dehydration, while allowing for wetting events to improve hydration above that achievable from soil water alone.

How plants may control water uptake through lenticels is unknown; however, we propose three mechanisms for future investigation. First, aquaporins have been implicated in both FWU (Laur & Hacke, 2014;

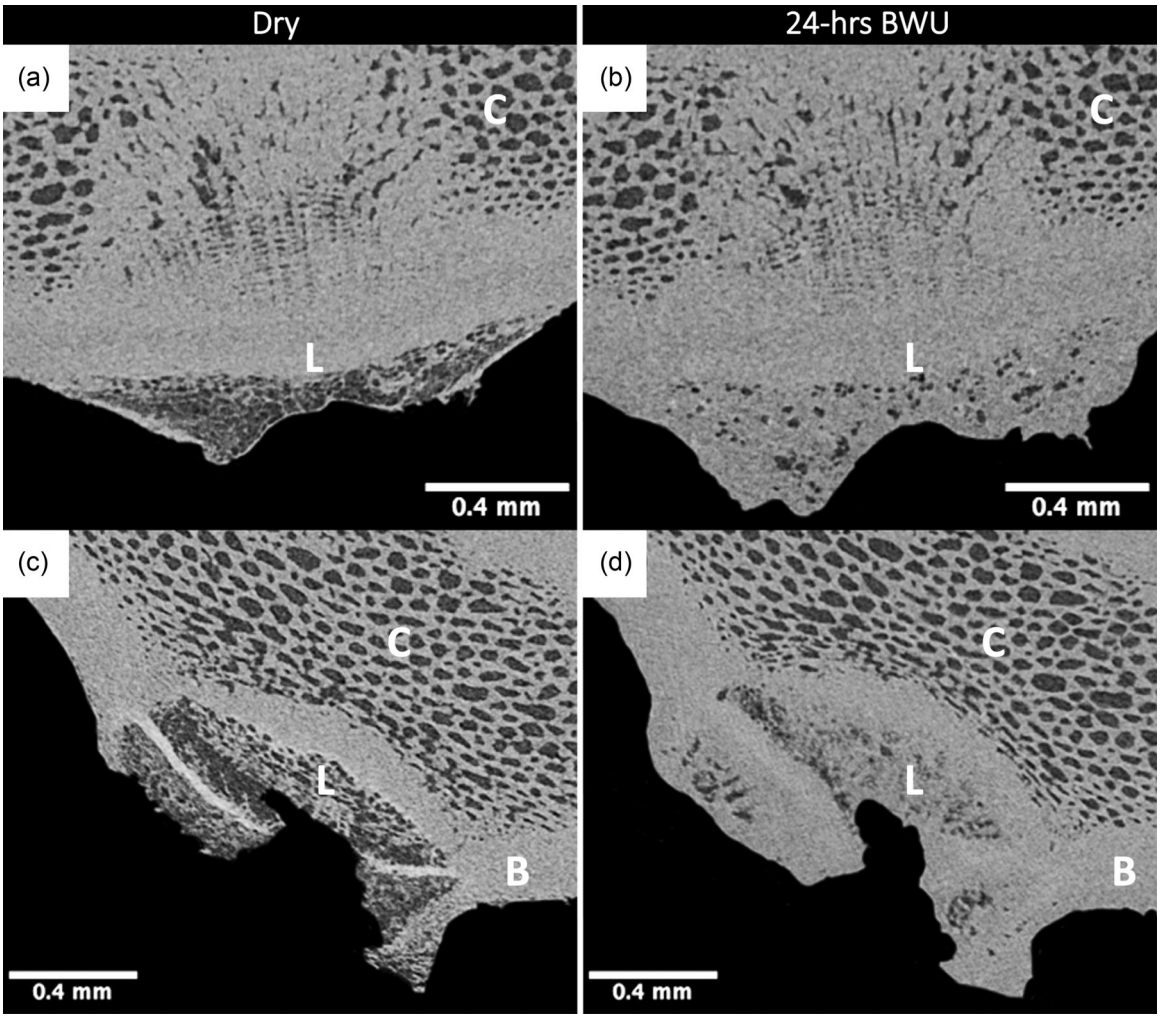

FIGURE 7 Enlarged view of lenticels from transverse XMCT sections of *Avicennia marina* subsp. *australasica* stems from Figure 6, showing lenticel structure swelling following 24 h of bark water uptake (24-h BWU). Each stem sample is shown in a pair of images (a,c) dry and (b,d) following 24-h BWU. Each image pair (a,b) and (c,d) was taken from a separate stem. Dark grey indicates gas spaces while light grey represents solid tissue and water. B, bark; C, cortex; L, lenticel; P, pith; V, vascular.

Ohrui et al., 2007; Tan et al., 2013; Vignesh & Palanisamy, 2021; Yan et al., 2015) and BWU (Mayr et al., 2014), by facilitating water transport across tissue membranes. Tan et al. (2013) found that aquaporins in salt-secretion glands of *Avicennia officinalis* could selectively reabsorb water, leaving salt behind. This has particular relevance for BWU in mangroves such as *A. marina* where stems may be periodically exposed to salt water. Hence, regulation of aquaporins may increase or decrease BWU and prevent solute entry during tidal inundation, providing a mechanism for selective BWU. Furthermore, aquaporins would provide a mechanism to explain our observation of transmembrane transport of fluorescein with liquid water from the lenticel pore, into the cortex and through the stem (Figure 2).

Alternatively, while waxes in the lenticel pore are believed to inhibit water movement into the lenticel (Lendzian, 2006), they may facilitate controlled uptake in a similar way to the modification of leaf cuticle permeability (Eller et al., 2013; Fernández et al., 2017; Rosado et al., 2010; Schreiber et al., 2001). Lastly, as with stomata, lenticels may have an opening and closing mechanism whereby swelling during wetting increases lenticel permeability and shrinkage during drying reduces permeability (Rosner & Morris, 2022). The observed lenticel swelling in XMCT experiments in response to wetting provides support for this mechanism, and would not leave the plant at increased risk of dehydration as it occurs under wet conditions. However, further investigation is required to determine if lenticel shrinkage and swelling affects BWU.

4.3 | Pathways for BWU are light enhanced but not light dependent

BWU occurred under both dark and light conditions. However, although not significant with a sample size of five stems ($p = 0.054$), there was a trend for mean values for BWU to increase when stems were exposed to light (Figure 5). This suggests that pathways for

TABLE 2 Change in stem tissues of *Avicennia marina* subsp. *australasica* dry and following 24-h of exposure to bark water uptake (24-h BWU).

Parameter	Unit	Mean difference ± SE *n* = 324-h BWU - Dry
Tissue radius		
Whole stem	mm	0.044 ± 0.002***
Bark	mm	0.039 ± 0.003***
Cortex	mm	0.020 ± 0.003***
Vascular	mm	−0.018 ± 0.003***
Pith	mm	0.002 ± 0.004
Tissue radius under lenticel		
Whole stem	mm	0.046 ± 0.010***
Bark	mm	0.043 ± 0.007***
Cortex	mm	0.021 ± 0.006**
Vascular	mm	−0.014 ± 0.004**
Pith	mm	−0.0036 ± 0.004
Lenticel characteristics		
Area	mm^2	0.098 ± 0.019***
Inner pore width	mm	−0.047 ± 0.138*
Outer pore width	mm	0.152 ± 0.028***
Height	mm	0.102 ± 0.014***

Note: Measurements were made on XMCT images taken dry and following 24-h BWU from three points along the stem length (slices) in each of the three stems. Radius of each slice was measured from the pith to three identical points on the outer bark around the stem diameter dry and following 24-h BWU to control for variation around the stem circumference and uneven swelling of stem tissues. Measurements for lenticel were made for every lenticel within each slice for each stem dry and following 24-h BWU Values are estimated marginal mean difference between 24-h BWU and dry ± SE from a linear mixed effects model with treatment as a fixed effect and random intercepts for individual, slice and measurement number within the slice. Tissue radius whole stem and lenticel inner pore width were log-transformed for analyses to account for nonnormality of model residuals. Corresponding observed means ± SE are given in Supporting Information: Table S7 and results from associated ANOVAs in Supporting Information: Table S8. Lenticels were observed to swell considerably in response to BWU (Figure 7). Tissue radius measurements were made on areas of the image where no lenticels were present (tissue radius) and directly underneath lenticels (tissue radius under lenticel) to control for effects of lenticel swelling. Tissue area measurements were calculated using radius measurements without lenticels to ensure changes to whole stem area were not artifacts of lenticel swelling.

*Significance codes: $p < 0.05$.

**$p < 0.01$. ***$p < 0.001$.

TABLE 3 Bark water uptake (BWU) characteristics of *Avicennia marina* subsp. *australasica* stems following 24 h of exposure to BWU.

Parameter	Unit	Mean ± SE *n* = 3
BWU characteristics		
Increase in water content	$g\ gDM^{-1}$	0.046 ± 0.0004
	$g\ m^2$	30.5 ± 2.0
	$g\ m^3$	17610.7 ± 877.6
Increase in water content (Relative to initial WC)	%	3.58 ± 0.17
Mean rate of water uptake	$g\ gDM^{-1}\ min^{-1}$	$0.000032 \pm 2.5 \times 10^{-7}$
	$g\ m^{-2}\ min^{-1}$	0.02 ± 0.001
	$g\ m^{-3}\ min^{-1}$	12.23 ± 0.61

Note: All values for BWU are based on total changes in stem WC over a 24-h period with normalisations based on stem dry mass, initial stem surface area, or volume. Values are mean ± SE.

Abbreviation: WC, water content.

BWU may involve light activation, but are not entirely light dependent. Liu et al. (2019) found that BWU and embolism repair increased under light conditions, proposing that light-induced corticular photosynthesis promoted water uptake, producing sugars that would decrease the osmotic potential of tissues within the stem. This would create a stronger ψ gradient for water movement from the bark surface into the inner stem tissue (Liu et al., 2019). Although here and in other studies, a high concentration of photosynthetic tissue was observed under lenticels (Kalachanis & Psaras, 2007; Manetas & Pfanz, 2005), if corticular photosynthesis generated greater ψ gradients that facilitated BWU through lenticels, then we should also have seen enhanced uptake with greater ψ gradients generated by mild dehydration as per Liu et al. (2019). Therefore, while corticular photosynthesis likely facilitates radial water transport and embolism repair within the stem, the role of corticular photosynthesis in BWU requires further investigation.

The hypothesised role of aquaporins in BWU would also provide a means to enhance BWU under light without BWU being light dependent. Studies have shown that aquaporin expression increases in response to light (Cochard et al., 2007; Hachez et al., 2008; Lopez et al., 2003; Yan et al., 2015). However, aquaporin expression can still occur under dark conditions (Yan et al., 2015). Therefore, aquaporins provide a mechanism by which BWU could be facilitated, controlled, and increased under light conditions, and should be investigated further.

4.4 | BWU caused swelling of bark and cortex tissues

The XMCT visualisation revealed tissue-dependent differences in the nature and extent of swelling. We found swelling of the cortex and bark in response to BWU such that the whole stem radius and area increased (Figure 6). Stem living tissues are believed to be the primary tissues for water storage, as their more elastic cell walls allow for greater changes in volume than more lignified cells (Pfautsch, Renard, et al., 2015). Therefore, swelling of the cortex following BWU implies filling of stem water storage tissues.

Unexpectedly, vascular tissue shrank in response to BWU, as swelling of bark and cortex tissues occurred radially in both directions increasing stem area and reducing vascular tissue area. Bulk

measurements of change in stem diameter likely underestimate the contribution of BWU to tissue swelling. Conversely, bulk or point dendrometer measurements of increased stem diameter could also overestimate the water storage of inner bark tissues because its expansion also increased the area of intercellular gas spaces (Figure 6). These results emphasise the importance of visualising tissues to understand the contributions that different tissues make to shrinking and swelling. In addition, we recorded significant swelling of lenticel tissue, where gas spaces were replaced by water in response to BWU (Figure 7). This swelling of outer lenticel tissue could provide a reservoir supporting continued BWU following a wetting event.

Discharge and recharge of stem water storage has been implicated in diel patterns of stem shrinkage and swelling. Water from storage tissue is discharged to the vascular tissue to support daily hydraulic function, and recharged following relaxation of tension in the xylem vessels (Pfautsch, Hölttä, et al., 2015). This occurs in response to transpiration driven ψ gradients (Nehemy et al., 2022; Sevanto et al., 2011; Steppe et al., 2012; Treydte et al., 2021; Zweifel et al., 2001), and phloem unloading changing osmotic potentials in cells (Mencuccini et al., 2013; Mencuccini et al., 2017; Pfautsch et al., 2015a; Sevanto et al., 2002, 2003, 2011; Zweifel et al., 2014). Therefore, swelling of the cortex suggests BWU during bark wetting events may contribute to diel patterns of stem swelling by recharging stem water storage tissues.

BWU recharge of stem water storage could play a significant role in the maintenance of stem WC and hydraulic function. Studies have found that internal water storage is slowly depleted as the dry season progresses (Preisler et al., 2022), and that extensive cell damage following the exhaustion of stored water prevented recovery from drought (Lamacque et al., 2020). Furthermore, decrease in stem diameter and diurnal fluctuations during drought preceded irreversible cessation of radial flow such that maintenance of radial flow was critical for drought recovery (Preisler et al., 2021). BWU during drought would improve hydration in the stem, preventing cellular damage where dehydration poses the greatest risk to stem and hence plant survival, even when wetting events may not be sufficient to improve hydration at the roots. Furthermore, although not observed here, BWU may provide a source of water to repair embolisms and buffer hydraulic conductivity (Katz et al., 1989; Liu et al., 2019; Mason Earles et al., 2016), enabling greater carbon gain and hydraulic safety.

The total amount of water uptake measured here was small, yet it was sufficient to increase the relative WC of the stems of *A. marina* by up to 3.7%. Using data from Fuenzalida et al. (2019), where $\psi_{salinity}$ was −1.71 MPa *A. marina* would have a hydration deficit of approximately 12% relative WC between $\psi_{salinity}$ and full hydration at 0 MPa. Therefore, BWU measured here would fill 31% of that hydration deficit. FWU in *A. marina* can increase ψ above those achievable through the roots (Coopman et al., 2021; Nguyen, Meir, Sack, et al., 2017), drive turgor-driven growth spurts (Schreel et al., 2019; Steppe et al., 2018), repair embolism (Fuenzalida, Blacker, et al., 2022), and sustain high rates of leaf transpiration for more than 120 min in high salinity environments (Nguyen, Meir, Sack, et al., 2017). Therefore, BWU co-occurring with FWU could immediately improve hydration where demand for water is greatest (Mason Earles et al., 2016). Indeed, exposure of shoots of *A. marina* to surface water led to overnight recovery of leaf hydraulic conductance (Fuenzalida et al., 2019), and reduced xylem tension for up to 7 h during transpiration (Coopman et al., 2021). However, Fuenzalida et al. (2019) and Coopman et al. (2021) did not distinguish between FWU and BWU and hence attributed recovery of hydraulic conductance to FWU. Nevertheless, we suggest that combined FWU and BWU would enable greater recovery than either could achieve alone and should be investigated in future studies.

4.5 | Limitations

The present XMCT experiment had limitations which, if improved upon, may reveal swelling of greater magnitude than were measured. Average uptake rates during XMCT closely resembled rates measured under dark conditions. Similarly, the total increase in WC on an area and volume basis over 24 h was comparable to results from 12 h of uptake in all experiments. Two possible explanations emerge.

First, it is possible that the majority of water uptake occurs in the first 12 h, and is sufficient to achieve full hydration in these small stems. However, these stems are hydraulically disconnected from roots and leaves. As such, we do not know how uptake would differ when water taken up through the bark could be redistributed throughout the plant. For example, studies have found that FWU not only increases hydration in the leaves, but was transported into stems, roots (Coopman et al., 2021; Steppe et al., 2018) and even into the soil (Cassana et al., 2016; Eller et al., 2013; Schreel et al., 2019).

Second, the light source used in XMCT experiments may not have been sufficient for light enhanced BWU. Due to the size constraints and temperature requirements of the XMCT chamber, only small household grow lights could be used. Furthermore, this experiment was conducted on small stems wrapped several times with paper towel, further reducing light reaching the stem. It is unlikely that stems in XMCT experiments received the same light exposure as in other BWU experiments. Rather, XMCT results likely reflect BWU under dark- or low-light conditions.

As discussed above, Liu et al. (2019) suggested that corticular photosynthesis facilitated embolism repair. In the present study, unrepaired embolism during BWU may be explained by insufficient light for corticular photosynthesis, or by insufficient rehydration to achieve the hydration levels required for refilling of embolised vessels. Future studies should aim to quantify BWU in whole plants, and the contribution of BWU to whole plant function under light and dark conditions.

5 | CONCLUSION

We showed for the first time that BWU occurs in stems of *A. marina* and was facilitated by lenticels on the outer bark surface. Lenticels provided a pathway for BWU that enhanced stem hydration while reducing the risks of unrestricted entry of saline water into the stem.

Further, swelling of stem tissues indicated that BWU contributes to recharge of stem water storage, the discharge of which is critical to daily stem function and survival during severe dehydration. The bark surface of a tree is present even when leaves are not, enabling controlled uptake of water during wetting events that are not sufficient to improve hydration at the roots. Further investigation into the role of BWU in the maintenance of whole plant hydration, especially during periods of water stress, is critical to understanding plant responses to increasing drought and salinity.

ACKNOWLEDGEMENTS

The authors acknowledge the Yuin, and the Ngunnawal and Ngambri peoples, the traditional custodians of the land on which this work was conducted. We pay our respects to them and their cultures and to elders both past and present. The authors thank the Australian Research Council for support through Discovery Project Grant DP180102969 awarded to Marilyn C. Ball. Holly A. A. Beckett was supported by Australian Government Research Training Program (RTP) Scholarships. The authors acknowledge the instruments and expertise of Microscopy Australia at the Centre for Advanced Microscopy, and the National Laboratory for X-ray Micro Computed Tomography at the Australian National University. These facilities are funded by the University and the Federal Government through NCRIS. The authors thank Matthew Bowes, Eldon Ball, John Passioura, Patrick Meir, and Danielle Way for thoughtful comments on the manuscript, and Tomás Fuenzalida for his care of the mangrove saplings. Open access publishing facilitated by Australian National University, as part of the Wiley - Australian National University agreement via the Council of Australian University Librarians.

DATA AVAILABILITY STATEMENT

The data that support the findings of this study are openly accessible at the Australian National University Data Commons. Available from: https://dx.doi.org/10.25911/654d-4c62.

ORCID

Holly A. A. Beckett http://orcid.org/0000-0001-9593-2430
Daryl Webb http://orcid.org/0000-0002-1494-9554
Adrian Sheppard http://orcid.org/0000-0001-9792-4143
Marilyn C. Ball http://orcid.org/0000-0001-9170-940X

REFERENCES

Abhik, S., Hope, P., Hendon, H.H., Hutley, L.B., Johnson, S., Drosdowsky, W. et al. (2021) Influence of the 2015–2016 El Niño on the record-breaking mangrove dieback along northern Australia coast. *Scientific Reports*, 11(1), 20411. Available from: https://doi.org/10.1038/s41598-021-99313-w

Allen, C.D., Macalady, A.K., Chenchouni, H., Bachelet, D., McDowell, N., Vennetier, M. et al. (2010) A global overview of drought and heat-induced tree mortality reveals emerging climate change risks for forests. *Forest Ecology and Management*, 259(4), 660–684. Available from: https://doi.org/10.1016/j.foreco.2009.09.001

Binks, O., Coughlin, I., Mencuccini, M. & Meir, P. (2020) Equivalence of foliar water uptake and stomatal conductance? *Plant, Cell & Environment*, 43(2), 524–528. Available from: https://doi.org/10.1111/pce.13663

Breshears, D.D., Adams, H.D., Eamus, D., McDowell, N.G., Law, D.J., Will, R.E. et al. (2013) The critical amplifying role of increasing atmospheric moisture demand on tree mortality and associated regional die-off. *Frontiers in Plant Science*, 4, 266. Available from: https://doi.org/10.3389/fpls.2013.00266

Bryant, C., Fuenzalida, T.I., Zavafer, A., Nguyen, H.T., Brothers, N., Harris, R.J. et al. (2021) Foliar water uptake via cork warts in mangroves of the Sonneratia genus. *Plant, Cell & Environment*, 44(9), 2925–2937. Available from: https://doi.org/10.1111/pce.14129

Burkhardt, J., Basi, S., Pariyar, S. & Hunsche, M. (2012) Stomatal penetration by aqueous solutions—an update involving leaf surface particles. *New Phytologist*, 196(3), 774–787. Available from: https://doi.org/10.1111/j.1469-8137.2012.04307.x

Cassana, F.F., Eller, C.B., Oliveira, R.S. & Dillenburg, L.R. (2016) Effects of soil water availability on foliar water uptake of *Araucaria angustifolia*. *Plant and Soil*, 399(1–2), 147–157. Available from: https://doi.org/10.1007/s11104-015-2685-0

Cochard, H., Venisse, J., Barigah, T., Brunel, N., Herbette, S., Guilliot, A. et al. (2007) Putative role of aquaporins in variable hydraulic conductance of leaves in response to light. *Plant Physiology*, 143(1), 122–133. Available from: https://doi.org/10.1104/pp.106.090092

Coopman, R.E., Nguyen, H.T., Mencuccini, M., Oliveira, R.S., Sack, L., Lovelock, C.E. et al. (2021) Harvesting water from unsaturated atmospheres: deliquescence of salt secreted onto leaf surfaces drives reverse sap flow in a dominant arid climate mangrove, *Avicennia marina*. *New Phytologist*, 231(4), 1401–1414. Available from: https://doi.org/10.1111/nph.17461

Dawson, T.E. & Goldsmith, G.R. (2018) The value of wet leaves. *New Phytologist*, 219(4), 1156–1169. Available from: https://doi.org/10.1111/nph.15307

Doughty, M.J. (2010) pH dependent spectral properties of sodium fluorescein ophthalmic solutions revisited. *Ophthalmic & Physiological Optics*, 30(2), 167–174. Available from: https://doi.org/10.1111/j.1475-1313.2009.00703.x

Duke, N.C., Kovacs, J.M., Griffiths, A.D., Preece, L., Hill, D.J.E., van Oosterzee, P. et al. (2017) Large-scale dieback of mangroves in Australia. *Marine and Freshwater Research*, 68(10), 1816–1829. Available from: https://doi.org/10.1071/MF16322

Eichert, T., Kurtz, A., Steiner, U. & Goldbach, H.E. (2008) Size exclusion limits and lateral heterogeneity of the stomatal foliar uptake pathway for aqueous solutes and water-suspended nanoparticles. *Physiologia Plantarum*, 134(1), 151–160. Available from: https://doi.org/10.1111/j.1399-3054.2008.01135.x

Eller, C.B., Lima, A.L. & Oliveira, R.S. (2013) Foliar uptake of fog water and transport belowground alleviates drought effects in the cloud forest tree species, *Drimys brasiliensis* (Winteraceae). *New Phytologist*, 199(1), 151–162. Available from: https://doi.org/10.1111/nph.12248

Fernández, V., Bahamonde, H.A., Javier Peguero-Pina, J., Gil-Pelegrín, E., Sancho-Knapik, D., Gil, L. et al. (2017) Physico-chemical properties of plant cuticles and their functional and ecological significance. *Journal of Experimental Botany*, 68(19), 5293–5306. Available from: https://doi.org/10.1093/jxb/erx302

Fox, J. & Weisberg, S. (2019) *An R companion to applied regression*. Third SAGE Publications. https://socialsciences.mcmaster.ca/jfox/Books/Companion/

Fuenzalida, T.I., Binks, O., Bryant, C.J., Wolfe, J. & Ball, M.C. (2022) Monitoring plant water status via static uniaxial compression of the leaf lamina. *Plant, Cell & Environment*, 45(9), 2589–2606. Available from: https://doi.org/10.1111/pce.14383

Fuenzalida, T.I., Blacker, M.J., Turner, M., Sheppard, A. & Ball, M.C. (2022) Foliar water uptake enables embolism removal in excised twigs of *Avicennia marina*. *The New Phytologist*, 237(4), 1136–1145. Available from: https://doi.org/10.1111/nph.18613

Fuenzalida, T.I., Bryant, C.J., Ovington, L.I., Yoon, H.J., Oliveira, R.S., Sack, L. et al. (2019) Shoot surface water uptake enables leaf hydraulic recovery in *Avicennia marina*. *New Phytologist*, 224(4), 1504–1511. Available from: https://doi.org/10.1111/nph.16126

Gil, A.M., Lopes, M.H., Pascoal Neto, C. & Callaghan, P.T. (2000) An NMR microscopy study of water absorption in cork. *Journal of Materials Science*, 35(8), 1891–1900. Available from: https://doi.org/10.1023/a:1004749932170

Graça, J. (2015) Suberin: the biopolyester at the frontier of plants. *Frontiers in Chemistry*, 3, 62. Available from: https://doi.org/10.3389/fchem.2015.00062

Grossiord, C., Buckley, T.N., Cernusak, L.A., Novick, K.A., Poulter, B., Siegwolf, R.T.W. et al. (2020) Plant responses to rising vapor pressure deficit. *New Phytologist*, 226(6), 1550–1566. Available from: https://doi.org/10.1111/nph.16485

Guzmán-Delgado, P., Laca, E. & Zwieniecki, M.A. (2021) Unravelling foliar water uptake pathways: the contribution of stomata and the cuticle. *Plant, Cell & Environment*, 44(6), 1728–1740. Available from: https://doi.org/10.1111/pce.14041

Hachez, C., Heinen, R.B., Draye, X. & Chaumont, F. (2008) The expression pattern of plasma membrane aquaporins in maize leaf highlights their role in hydraulic regulation. *Plant Molecular Biology*, 68(4–5), 337–353. Available from: https://doi.org/10.1007/s11103-008-9373-x

Harris, R.M.B., Beaumont, L.J., Vance, T.R., Tozer, C.R., Remenyi, T.A., Perkins-Kirkpatrick, S.E. et al. (2018) Biological responses to the press and pulse of climate trends and extreme events. *Nature Climate Change*, 8(7), 579–587. Available from: https://doi.org/10.1038/s41558-018-0187-9

Hayes, M.A., Chapman, S., Jesse, A., O'Brien, E., Langley, J.A., Bardou, R. et al. (2020) Foliar water uptake by coastal wetland plants: a novel water acquisition mechanism in arid and humid subtropical mangroves. *Journal of Ecology*, 108(6), 2625–2637. Available from: https://doi.org/10.1111/1365-2745.13398

Hoberman, C. (1990) Reversibly expandable doubly-curved truss structure. *US Patent*. https://patentimages.storage.googleapis.com/e0/83/93/c4ddb2fa7ca5bb/US4942700.pdf.

van den Honert, T.H. (1948) Water transport in plants as a catenary process. *Discussions of the Faraday Society*, 3(0), 146–153. Available from: https://doi.org/10.1039/DF9480300146

Kalachanis, D. & Psaras, G.K. (2007) Structural changes in primary lenticels of *Olea Europaea* and Cercis Siliquastrum during the year. *IAWA Journal*, 28(4), 445–456. Available from: https://doi.org/10.1163/22941932-90001654

Katz, C., Oren, R., Schulze, E.-D. & Milburn, J.A. (1989) Uptake of water and solutes through twigs of *Picea abies* (L.) karst. *Trees*, 3(1), 33–37. Available from: https://doi.org/10.1007/BF00202398

Kingston, A.M., Myers, G.R., Latham, S.J., Recur, B., Li, H. & Sheppard, A.P. (2018) Space-filling X-ray source trajectories for efficient scanning in large-angle cone-beam computed tomography. *IEEE Transactions on Computational Imaging*, 4(3), 447–458. Available from: https://doi.org/10.1109/TCI.2018.2841202

Kuznetsova, A., Brockhoff, P.B. & Christensen, R.H.B. (2017) lmerTest Package: Tests in Linear Mixed Effects Models. *Journal of statistical software*, 82(13), 1–26. Available from: https://doi.org/10.18637/jss.v082.i13

Lamacque, L., Charrier, G., Farnese, F.S., Lemaire, B., Améglio, T. & Herbette, S. (2020) Drought-induced mortality: branch diameter variation reveals a point of no recovery in lavender species. *Plant Physiology*, 183(4), 1638–1649. Available from: https://doi.org/10.1104/pp.20.00165

Latham, S.J., Varslot, T. & Sheppard, A. (2008) Automated registration for augmenting micro-CT 3D images. *ANZIAM Journal*, 50, 534. Available from: https://doi.org/10.21914/anziamj.v50i0.1389

Laur, J. & Hacke, U.G. (2014) Exploring *Picea glauca* aquaporins in the context of needle water uptake and xylem refilling. *New Phytologist*, 203(2), 388–400. Available from: https://doi.org/10.1111/nph.12806

Lendzian, K.J. (2006) Survival strategies of plants during secondary growth: barrier properties of phellems and lenticels towards water, oxygen, and carbon dioxide. *Journal of Experimental Botany*, 57(11), 2535–2546. Available from: https://doi.org/10.1093/jxb/erl014

Lenth, R.V. (2020) *emmeans: estimated marginal means, aka least-squares means*. https://CRAN.R-project.org/package=emmeans.

Liu, J., Gu, L., Yu, Y., Huang, P., Wu, Z., Zhang, Q. et al. (2019) Corticular photosynthesis drives bark water uptake to refill embolized vessels in dehydrated branches of *Salix matsudana*. *Plant, Cell & Environment*, 42(9), 2584–2596. Available from: https://doi.org/10.1111/pce.13578

Lopez, F., Bousser, A., Sissoëff, I., Gaspar, M., Lachaise, B., Hoarau, J. et al. (2003) Diurnal regulation of water transport and aquaporin gene expression in maize roots: contribution of PIP2 proteins. *Plant & Cell Physiology*, 44(12), 1384–1395. Available from: https://doi.org/10.1093/pcp/pcg168

Losso, A., Bär, A., Unterholzner, L., Bahn, M. & Mayr, S. (2021) Branch water uptake and redistribution in two conifers at the alpine treeline. *Scientific Reports*, 11(1), 22560. Available from: https://doi.org/10.1038/s41598-021-00436-x

Lovelock, C.E., Feller, I.C., Reef, R., Hickey, S. & Ball, M.C. (2017) Mangrove dieback during fluctuating sea levels. *Scientific Reports*, 7(1), 1680. Available from: https://doi.org/10.1038/s41598-017-01927-6

Lucas, R., Finlayson, C.M., Bartolo, R., Rogers, K., Mitchell, A., Woodroffe, C.D. et al. (2018) Historical perspectives on the mangroves of Kakadu National Park. *Marine & Freshwater Research*, 69(7), 1047. Available from: https://doi.org/10.1071/mf17065

Manetas, Y. & Pfanz, H. (2005) Spatial heterogeneity of light penetration through periderm and lenticels and concomitant patchy acclimation of corticular photosynthesis. *Trees*, 19(4), 409–414. Available from: https://doi.org/10.1007/s00468-004-0399-7

Mason Earles, J., Sperling, O., Silva, L.C., McElrone, A.J., Brodersen, C.R., North, M.P. et al. (2016) Bark water uptake promotes localized hydraulic recovery in coastal redwood crown. *Plant, Cell & Environment*, 39(2), 320–328. Available from: https://doi.org/10.1111/pce.12612

Matsunaga, H., Matsuo, N., Nakai, T., Yoshifuji, N., Tanaka, N., Tanaka, K. et al. (2021) Absorption and emission of water vapor from the bark of teak (*Tectona grandis*), a deciduous tree, in a tropical region during the dry season. *Hydrological Research Letters*, 15(3), 58–63. Available from: https://doi.org/10.3178/hrl.15.58

Mayr, S., Schmid, P., Laur, J., Rosner, S., Charra-Vaskou, K., Dämon, B. et al. (2014) Uptake of water via branches helps timberline conifers refill embolized xylem in late winter. *Plant Physiology*, 164(4), 1731–1740. Available from: https://doi.org/10.1104/pp.114.236646

McDowell, N.G., Sapes, G., Pivovaroff, A., Adams, H.D., Allen, C.D. et al. (2022) Mechanisms of woody-plant mortality under rising drought, CO2 and vapour pressure deficit. *Nature Reviews Earth & Environment*, 3(5), 294–308. Available from: https://doi.org/10.1038/s43017-022-00272-1

Meinzer, F.C., Woodruff, D.R., Domec, J.-C., Goldstein, G., Campanello, P.I., Gatti, M.G. et al. (2008) Coordination of leaf and stem water transport properties in tropical forest trees. *Oecologia*, 156(1), 31–41. Available from: https://doi.org/10.1007/s00442-008-0974-5

Mencuccini, M., Hölttä, T., Sevanto, S. & Nikinmaa, E. (2013) Concurrent measurements of change in the bark and xylem diameters of trees reveal a phloem-generated turgor signal. *New Phytologist*, 198(4), 1143–1154. Available from: https://doi.org/10.1111/nph.12224

Mencuccini, M., Salmon, Y., Mitchell, P., Hölttä, T., Choat, B., Meir, P. et al. (2017) An empirical method that separates irreversible stem radial growth from bark water content changes in trees: theory and case studies. *Plant, Cell & Environment*, 40(2), 290–303. Available from: https://doi.org/10.1111/pce.12863

Moon, G., Clough, B., Peterson, C. & Allaway, W. (1986) Apoplastic and symplastic pathways in *Avicennia marina* (Forsk.) Vierh. roots

revealed by fluorescent tracer dyes. *Functional Plant Biology*, 13(5), 637–648. Available from: https://doi.org/10.1071/pp9860637

Morrisey, D.J., Swales, A., Dittmann, S., Morrison, M.A., Lovelock, C.E. & Beard, C.M. (2010) The ecology and management of temperate mangroves. In: *Oceanography and marine biology*. Chapman and Hall/CRC. pp. 43–160. https://doi.org/10.1201/ebk1439821169-2

Myers, G.R., Kingston, A.M., Varslot, T.K. & Sheppard, A.P. (2011) Extending reference scan drift correction to high-magnification high-cone-angle tomography. *Optics Letters*, 36(24), 4809–4811. Available from: https://doi.org/10.1364/OL.36.004809

Nehemy, M.F., Benettin, P., Allen, S.T., Steppe, K., Rinaldo, A. & Lehmann, M.M. et al. (2022) Phloem water isotopically different to xylem water: potential causes and implications for ecohydrological tracing. *Ecohydrology*, 15(3), e2417. Available from: https://doi.org/10.1002/eco.2417

Nguyen, H.T., Meir, P., Sack, L., Evans, J.R., Oliveira, R.S. & Ball, M.C. (2017) Leaf water storage increases with salinity and aridity in the mangrove *Avicennia marina*: integration of leaf structure, osmotic adjustment and access to multiple water sources. *Plant, Cell & Environment*, 40(8), 1576–1591. Available from: https://doi.org/10.1111/pce.12962

Nguyen, H.T., Meir, P., Wolfe, J., Mencuccini, M. & Ball, M.C. (2017) Plumbing the depths: extracellular water storage in specialized leaf structures and its functional expression in a three-domain pressure-volume relationship. *Plant, Cell & Environment*, 40(7), 1021–1038. Available from: https://doi.org/10.1111/pce.12788

Ohrui, T., Nobira, H., Sakata, Y., Taji, T., Yamamoto, C., Nishida, K. et al. (2007) Foliar trichome- and aquaporin-aided water uptake in a drought-resistant epiphyte Tillandsia ionantha Planchon. *Planta*, 227(1), 47–56. Available from: https://doi.org/10.1007/s00425-007-0593-0

Oparka, K.J. (1991) Uptake and compartmentation of fluorescent probes by plant cells. *Journal of Experimental Botany*, 42(5), 565–579. Available from: https://doi.org/10.1093/jxb/42.5.565

Pfautsch, S., Hölttä, T. & Mencuccini, M. (2015) Hydraulic functioning of tree stems--fusing ray anatomy, radial transfer and capacitance. *Tree Physiology*, 35(7), 706–722. Available from: https://doi.org/10.1093/treephys/tpv058

Pfautsch, S., Renard, J., Tjoelker, M.G. & Salih, A. (2015) Phloem as capacitor: radial transfer of water into xylem of tree stems occurs via symplastic transport in ray parenchyma. *Plant Physiology*, 167(3), 963–971. Available from: https://doi.org/10.1104/pp.114.254581

Preisler, Y., Hölttä, T., Grünzweig, J.M., Oz, I., Tatarinov, F., Ruehr, N.K. et al. (2022) The importance of tree internal water storage under drought conditions. *Tree Physiology*, 42(4), 771–783. Available from: https://doi.org/10.1093/treephys/tpab144

Preisler, Y., Tatarinov, F., Grünzweig, J.M. & Yakir, D. (2021) Seeking the 'point of no return' in the sequence of events leading to mortality of mature trees. *Plant, Cell & Environment*, 44(5), 1315–1328. Available from: https://doi.org/10.1111/pce.13942

R Core Team. (2023) *R: a language and environment for statistical computing*. R Foundation for Statistical Computing. https://www.R-project.org/

Reef, R., Ball, M.C. & Lovelock, C.E. (2012) The impact of a locust plague on mangroves of the arid Western Australia coast. *Journal of tropical ecology*, 28(3), 307–311. Available from: https://doi.org/10.1017/S0266467412000041

Rosado, B.H.P., Oliveira, R.S. & Marinho Aidar, M.P. (2010) Is leaf water repellency related to vapor pressure deficit and crown exposure in tropical forests? *Acta Oecologica*, 36(6), 645–649. Available from: https://doi.org/10.1016/j.actao.2010.10.001

Rosner, S. & Morris, H. (2022) Breathing life into trees: the physiological and biomechanical functions of lenticels. *IAWA Journal*, 43(3), 234–262. Available from: https://doi.org/10.1163/22941932-bja10090

Schaepdryver, K.H.D., Goossens, W., Naseef, A., Kalpuzha Ashtamoorthy, S. & Steppe, K. (2022) Foliar water uptake capacity in six mangrove species. *Forests*, 13(6), 951. Available from: https://doi.org/10.3390/f13060951

Schindelin, J., Arganda-Carreras, I., Frise, E., Kaynig, V., Longair, M., Pietzsch, T. et al. (2012) Fiji: an open-source platform for biological-image analysis. *Nature Methods*, 9(7), 676–682. Available from: https://doi.org/10.1038/nmeth.2019

Scholander, P.F., Hammel, H.T., Hemmingsen, E.A. & Bradstreet, E.D. (1964) Hydrostatic pressure and osmotic potential in leaves of mangroves and some other plants. *Proceedings of the National Academy of Sciences*, 52(1), 119–125. Available from: https://doi.org/10.1073/pnas.52.1.119

Schreel, J.D.M. & Steppe, K. (2020) Foliar water uptake in trees: negligible or necessary? *Trends in Plant Science*, 25(6), 590–603. Available from: https://doi.org/10.1016/j.tplants.2020.01.003

Schreel, J.D.M., Van de Wal, B.A.E., Hervé-Fernandez, P., Boeckx, P. & Steppe, K. (2019) Hydraulic redistribution of foliar absorbed water causes turgor-driven growth in mangrove seedlings. *Plant, Cell & Environment*, 42(8), 2437–2447. Available from: https://doi.org/10.1111/pce.13556

Schreiber, L., Skrabs, M., Hartmann, K., Diamantopoulos, P., Simanova, E. & Santrucek, J. (2001) Effect of humidity on cuticular water permeability of isolated cuticular membranes and leaf disks. *Planta*, 214(2), 274–282. Available from: https://doi.org/10.1007/s004250100615

Schönherr, J. & Ziegler, H. (1980) Water permeability of Betula periderm. *Planta*, 147(4), 345–354. Available from: https://doi.org/10.1007/BF00379844

Scoffoni, C. & Sack, L. (2017) The causes and consequences of leaf hydraulic decline with dehydration. *Journal of Experimental Botany*, 68(16), 4479–4496. Available from: https://doi.org/10.1093/jxb/erx252

Serra, O., Mähönen, A.P., Hetherington, A.J. & Ragni, L. (2022) The making of plant armor: the periderm. *Annual Review of Plant Biology*, 73, 405–432. Available from: https://doi.org/10.1146/annurev-arplant-102720-031405

Sevanto, S., Hölttä, T. & Holbrook, N.M. (2011) Effects of the hydraulic coupling between xylem and phloem on diurnal phloem diameter variation. *Plant, Cell & Environment*, 34(4), 690–703. Available from: https://doi.org/10.1111/j.1365-3040.2011.02275.x

Sevanto, S., Vesala, T., Perämäki, M. & Nikinmaa, E. (2002) Time lags for xylem and stem diameter variations in a Scots pine tree. *Plant, Cell & Environment*, 25(8), 1071–1077. Available from: https://doi.org/10.1046/j.1365-3040.2002.00884.x

Sevanto, S., Vesala, T., Perämäki, M. & Nikinmaa, E. (2003) Sugar transport together with environmental conditions controls time lags between xylem and stem diameter changes. *Plant, Cell & Environment*, 26(8), 1257–1265. Available from: https://doi.org/10.1046/j.1365-3040.2003.01049.x

Simonin, K.A., Santiago, L.S. & Dawson, T.E. (2009) Fog interception by *Sequoia sempervirens* (D. Don) crowns decouples physiology from soil water deficit. *Plant, Cell & Environment*, 32(7), 882–892. Available from: https://doi.org/10.1111/j.1365-3040.2009.01967.x

Van Stan, J.T., Dymond, S.F. & Klamerus-Iwan, A. (2021) Bark-water interactions across ecosystem states and fluxes. *Frontiers in Forests and Global Change*, 4, 660662. Available from: https://doi.org/10.3389/ffgc.2021.660662

Steppe, K., Cochard, H., Lacointe, A. & Améglio, T. (2012) Could rapid diameter changes be facilitated by a variable hydraulic conductance? *Plant, Cell & Environment*, 35(1), 150–157. Available from: https://doi.org/10.1111/j.1365-3040.2011.02424.x

Steppe, K., Vandegehuchte, M.W., Van de Wal, B.A.E., Hoste, P., Guyot, A., Lovelock, C.E. et al. (2018) Direct uptake of canopy rainwater causes turgor-driven growth spurts in the mangrove *Avicennia marina*. *Tree Physiology*, 38(7), 979–991. Available from: https://doi.org/10.1093/treephys/tpy024

Tan, W.-K., Lin, Q., Lim, T.-M., Kumar, P. & Loh, C.-S. (2013) Dynamic secretion changes in the salt glands of the mangrove tree species

Avicennia officinalis in response to a changing saline environment. *Plant, Cell & Environment*, 36(8), 1410–1422. Available from: https://doi.org/10.1111/pce.12068

Tomasella, M., Natale, S., Petruzzellis, F., Di Bert, S., D'Amico, L., Tromba, G. et al. (2022) No evidence for light-induced embolism repair in cut stems of drought-resistant Mediterranean species under soaking. *Plants*, 11(3), 307. Available from: https://doi.org/10.3390/plants11030307

Treydte, K., Lehmann, M.M., Wyczesany, T. & Pfautsch, S. (2021) Radial and axial water movement in adult trees recorded by stable isotope tracing. *Tree Physiology*, 41(12), 2248–2261. Available from: https://doi.org/10.1093/treephys/tpab080

Trifiló, P., Raimondo, F., Savi, T., Lo Gullo, M.A. & Nardini, A. (2016) The contribution of vascular and extra-vascular water pathways to drought-induced decline of leaf hydraulic conductance. *Journal of Experimental Botany*, 67(17), 5029–5039. Available from: https://doi.org/10.1093/jxb/erw268

Varslot, T., Kingston, A., Myers, G. & Sheppard, A. (2011) High-resolution helical cone-beam micro-CT with theoretically-exact reconstruction from experimental data. *Medical Physics*, 38(10), 5459–5476. Available from: https://doi.org/10.1118/1.3633900

Vesala, T., Sevanto, S., Grönholm, T., Salmon, Y., Nikinmaa, E., Hari, P. et al. (2017) Effect of leaf water potential on internal humidity and CO_2 dissolution: reverse transpiration and improved water use efficiency under negative pressure. *Frontiers in Plant Science*, 8, 54. Available from: https://doi.org/10.3389/fpls.2017.00054

Vignesh, M.R. & Palanisamy, S. (2021) Aquaporin and its effect on foliar uptake to overcome drought stress in plants. *Plant Physiology Reports*, 26(2), 193–199. Available from: https://doi.org/10.1007/s40502-021-00567-3

Wickham, H. (2016) *ggplot2: elegant graphics for data analysis*. New York: Springer-Verlag. https://ggplot2.tidyverse.org

Wolfe, B.T. (2020) Bark water vapour conductance is associated with drought performance in tropical trees. *Biology Letters*, 16, 20200263. Available from: https://doi.org/10.1098/rsbl.2020.0263

Wolfe, B.T., Sperry, J.S. & Kursar, T.A. (2016) Does leaf shedding protect stems from cavitation during seasonal droughts? A test of the hydraulic fuse hypothesis. *New Phytologist*, 212(4), 1007–1018. Available from: https://doi.org/10.1111/nph.14087

Yan, X., Zhou, M., Dong, X., Zou, S., Xiao, H. & Ma, X.-F. (2015) Molecular mechanisms of foliar water uptake in a desert tree. *AoB Plants*, 7, plv129. Available from: https://doi.org/10.1093/aobpla/plv129

Yáñez-Espinosa, L. & Angeles, G. (2022) Does mangrove stem bark have an internal pathway for gas flow? *Trees*, 36(1), 361–377. Available from: https://doi.org/10.1007/s00468-021-02210-y

Zweifel, R., Drew, D.M., Schweingruber, F. & Downes, G.M. (2014) Xylem as the main origin of stem radius changes in Eucalyptus. *Functional Plant Biology*, 41(5), 520–534. Available from: https://doi.org/10.1071/FP13240

Zweifel, R., Item, H. & Hasler, R. (2001) Link between diurnal stem radius changes and tree water relations. *Tree Physiology*, 21(12–13), 869–877. Available from: https://doi.org/10.1093/treephys/21.12-13.869

SUPPORTING INFORMATION

Additional supporting information can be found online in the Supporting Information section at the end of this article.

How to cite this article: Beckett, H. A. A., Webb, D., Turner, M., Sheppard, A. & Ball, M. C. (2024) Bark water uptake through lenticels increases stem hydration and contributes to stem swelling. *Plant, Cell & Environment*, 47, 72–90. https://doi.org/10.1111/pce.14733